# The canonical PilT retraction ATPase promotes both extension and retraction of the MSHA type IVa pilus in *Vibrio cholerae*

Hannah Q. Hughes[1], Triana N. Dalia[1], Courtney K. Ellison[1,2], and Ankur B. Dalia[1,*].

[1]Department of Biology, Indiana University, Bloomington, IN
[2]Present address: Department of Microbiology, University of Georgia, Athens, GA
*Author for correspondence: ankdalia@indiana.edu

## ABSTRACT

Diverse bacterial species use type IVa pili (T4aP) to interact with their environments. The dynamic extension and retraction of T4aP is critical for their function, but the mechanisms that regulate this dynamic activity remain poorly understood. T4aP are typically extended via the activity of a dedicated extension motor ATPase and retracted via the action of an antagonistic retraction motor ATPase called PilT. These motors are generally functionally independent, and loss of PilT commonly results in T4aP hyperpiliation due to undeterred pilus extension. However, for the mannose-sensitive hemagglutinin (MSHA) T4aP of *Vibrio cholerae*, the loss of PilT results in a loss of surface piliation, which is unexpected based on our current understanding of T4aP dynamics. Here, we employ a combination of genetic and cell biological approaches to dissect the underlying mechanism. Our results demonstrate that PilT is necessary for MSHA pilus extension in addition to its well-established role in promoting MSHA pilus retraction. Through a suppressor screen, we also provide genetic evidence that the structure of the MshA major pilin contributes to pilus extension. Together, these findings contribute to our understanding of the factors that regulate pilus extension and describe a previously uncharacterized function for the PilT motor ATPase.

## AUTHOR SUMMARY

Many bacteria use filamentous appendages called pili to interact with their environment. These fibers dynamically extend and retract through the activity of ATPase motor proteins. In most pilus systems, deletion of the retraction motor results in uninterrupted pilus extension, leading to hyperpiliation. However, in the MSHA pilus system of *V. cholerae*, deletion of the retraction motor, *pilT*, results in a decrease in the number of surface pili. Here, we show that PilT is unexpectedly required for MSHA pilus extension in addition to its defined role in promoting pilus retraction. These results extend our understanding of the complex mechanisms underlying the dynamic activity of these broadly conserved filamentous appendages.

## INTRODUCTION

Type IVa pili (T4aP) are used by a wide range of bacteria to interact with their environment [1]. These fibers extend and retract from cell surfaces to accomplish a wide range of behaviors, including twitching motility [2, 3], the uptake of DNA during natural transformation [4, 5], and initial attachment of cells to a surface [6-8]. The frequency of pilus dynamic activity and the number of surface pili maintained at any given time directly impacts the ability of the cell to perform pilus-related functions. For example, the *Neisseria meningitidis* pilus system has been characterized to perform different functions based on the number of surface pili, ranging from DNA uptake, where a single pilus is sufficient, to interaction with host cells, which optimally

requires five pili [9]. Elucidating the regulation of pilus dynamic activity and pilus number is therefore crucial to understanding pilus function.

T4aP are primarily composed of repeating subunits of the major pilin, which are extruded from the inner membrane and assembled into a filament through the activity of a dedicated extension ATPase. The process is reversed through the activity of a retraction ATPase, commonly called PilT, which deposits major pilins back into the inner membrane pool [10]. In these dynamic pilus systems, the activity of the extension and retraction motors plays an important role in regulating surface piliation. Current models propose that these motors compete to interact with the T4aP pilus machine, such that the motor that interacts with the platform dictates the direction of dynamic activity [11, 12]. If the extension motor is inhibited, pilus retraction dominates and pilus number decreases [13-15]. Conversely, if the retraction motor is disrupted, extension occurs undeterred, resulting in hyperpiliation [5, 16-19]. However, these trends are not universally observed, indicating that alternate mechanisms of pilus regulation exist and contribute to surface piliation.

Deletion of *pilT* does not result in hyperpiliation of the T4P in *Francisella tularensis* [20], *Clostridium perfringens* [21], or *V. cholerae* mannose-sensitive hemagglutinin (MSHA) pili [22-25]. Indeed, for each of these systems, deletion of *pilT* results in a decrease in piliation. This observation is counterintuitive based on our current understanding of T4aP and suggests that T4aP dynamic activity is likely regulated by more than a simple competition between extension and retraction motors. In this study, we use the MSHA T4aP of *V. cholerae* as a model system to investigate PilT-dependent surface piliation because of the extensive genetic and cell biological tools that have recently been developed to study the dynamic activity of these pili [7, 22, 25-27].

## RESULTS

*Vibrio cholerae* expresses two distinct T4aP systems: MSHA pili and competence pili (also known as ChiRP pili). MSHA pili facilitate biofilm formation by promoting the initial attachment of cells to a surface [8, 28-30], while competence pili promote DNA uptake for horizontal gene transfer by natural transformation [31, 32]. The dynamic activity of both T4aP systems can be studied in live cells via the use of a major pilin cysteine knock-in mutation (*mshA*$^{T70C}$ for MSHA pili; *pilA*$^{S67C}$ for competence pili) and subsequent labeling with thiol-reactive fluorescent maleimide dyes [7, 26, 31]. While these T4aP have distinct extension motor ATPases (MshE for MSHA pili; PilB for competence pili), they both rely on the same retraction ATPase, PilT, for efficient retraction (**Fig. 1A-B**). Deletion of *pilT*, however, exhibits distinct effects on these two T4aP systems. Loss of *pilT* results in a marked increase in the number of surface competence pili, which is consistent with unregulated extension in this background as observed in many other T4aP systems [14, 33-36]. Conversely, the loss of PilT dramatically reduces the number of MSHA pili (**Fig. 1B-C**). In fact, in the Δ*pilT* mutant, most cells lack MSHA pili, and the rare cells that do make pili generally display a single pilus that is longer than those observed in the parent (**Fig. 1B-C**). These results are consistent with multiple prior studies [15, 22-25, 31].

One model that has been proposed for the observed reduction in MSHA surface piliation is that PilT is necessary to disrupt pilus extension after it is initiated [25]. Thus, in Δ*pilT* cells, a single MSHA T4aP machine undergoes uncontrolled “runaway” extension that exhausts the MshA major pilin pool of the cell. This is consistent with the markedly longer pili observed in the piliated Δ*pilT* cells (**Fig. 1B**). This model predicts that a similar proportion of cells should be piliated in both the parent and Δ*pilT* strains because initiation of pilus extension should not be

affected. However, the Δ*pilT* strain shows a 4-fold reduction in the percentage of piliated cells (**Fig. 1C**). One possible explanation for this discrepancy could be that the long MSHA pili in the Δ*pilT* cells are sheared off during the pilus labeling process. If runaway extension was followed by shearing and loss of surface pili, we would expect Δ*pilT* cells to exhibit a 4-fold reduction in the level of cell-associated MshA major pilin. However, Western blot analysis indicates that cell-associated MshA major pilin is similar in the parent and Δ*pilT* strains (**Fig. 2A**). In the T4aP systems of *Pseudomonas aeruginosa* and *Myxococcus xanthus*, major pilin expression is increased in Δ*pilT* cells due to feedback regulation by the PilS-PilR two-component system [37, 38]. *V. cholerae* lacks homologs of the PilS-PilR system, but it remains possible that Δ*pilT* cells also compensate for the loss of sheared pili by increasing expression of MshA major pilin. If so, the total amount of major pilins present in the cells + supernatant (*i.e.*, unassembled + assembled, shed pili) should be markedly increased in the Δ*pilT* strain compared to the parent. However, we found that MshA protein levels were similar in the parent and Δ*pilT* samples even when the supernatants were included (**Fig. 2A**). These results are not consistent with runaway extension of MSHA pili in Δ*pilT* cells. Instead, we next assessed whether cells had failed to assemble MSHA pili in the Δ*pilT* background. The Alexa Fluor 488-maleimide dye (AF488-mal) used to fluorescently label cysteine modified MshA major pilins ($MshA^{T70C}$) can pass through the outer membrane of *V. cholerae* and label pilins retained in the inner membrane. Thus, the cell body fluorescence of labeled cells can serve as a proxy for the concentration of unassembled major pilins. A Δ*mshE* mutant, which cannot assemble MSHA pili, was used as a control to demonstrate the cell body fluorescence of a strain that retains all of its MshA major pilins in the inner membrane. Also, a strain that lacks the $mshA^{T70C}$ mutation (*i.e.*, unlabelable) was included to indicate the background fluorescence observed in the absence of any labelable major pilins. We found that the cell body fluorescence of unpiliated AF488-mal labeled Δ*pilT* cells was more similar to the Δ*mshE* strain than to the unlabelable strain (**Fig. 2B**), indicating that unpiliated Δ*pilT* cells retain a significant concentration of MshA in their inner membrane. Together, these data suggest that the majority of Δ*pilT* cells fail to assemble MSHA pili.

A lack of pilus biogenesis in the Δ*pilT* background could be due to an indirect downregulation of MshE extension motor activity. If so, we hypothesized that increased expression of *mshE* should recover surface piliation in the Δ*pilT* mutant. Overexpression of *mshE*, however, did not recover piliation in the Δ*pilT* background (**Fig. S1**). MshE activity is also allosterically regulated by cyclic-di-GMP (c-di-GMP), such that high levels of c-di-GMP stimulate MshE-dependent pilus extension [22, 39]. Thus, the lack of MSHA biogenesis in Δ*pilT* cells could be due to a decrease in cellular levels of c-di-GMP, diminishing MshE activity. To test this, we increased the intracellular concentration of c-di-GMP in Δ*pilT* cells by overexpressing a previously characterized diguanylate cyclase, DcpA [40]. Elevated c-di-GMP also induces expression of the *vps* and *rbm* loci [41], which encode *Vibrio* polysaccharide and biofilm matrix proteins, respectively. To avoid cell clumping due to the expression of these biofilm factors and for ease of pilus quantification in these experiments, we deleted both the *vps* and *rbm* loci (ΔVC0917-VC0939; here called Δ*vps*) in the background where *dcpA* was overexpressed. We found that overexpression of *dcpA* was insufficient to restore piliation in the Δ*pilT* background (**Fig. S1**). To further test whether c-di-GMP was involved in regulating MSHA piliation in the Δ*pilT* background, we took advantage of a previously-characterized allele of *mshE* – $mshE^{L10A/L54AL/58A}$ (denoted here as *mshE**) – that genetically mimics the c-di-GMP bound state of MshE and promotes MSHA extension independently of c-di-GMP concentration [27, 39]. Native expression and overexpression of *mshE**, however, both failed to overcome the MSHA

surface piliation defect of the Δ*pilT* background (**Fig. S1**). These results suggest that PilT does not promote MSHA biogenesis by indirectly affecting MshE activity.

Because PilT did not indirectly alter MSHA biogenesis through downregulation of the two factors known to influence extension (MshE and c-di-GMP), we hypothesized that PilT actively participates in MSHA biogenesis. If this were true, we would expect Δ*pilT* cells to extend MSHA pili very rapidly following PilT induction. To test this, we generated strains where *pilT* expression could be tightly controlled via an arabinose- and theophylline-inducible ectopic expression construct [42] ($P_{BAD}$-ribo-*pilT*), and we measured piliation in cells before and after induction of the ectopic *pilT* construct. While only minor changes in piliation were observed in a strain still expressing native *pilT*, induction of ectopic *pilT* in the Δ*pilT* background rapidly recovered piliation to parental levels (**Fig. 3A-B**). This increase was not observed in strains lacking the $P_{BAD}$-ribo-*pilT* construct, indicating that this response was not due to a nonspecific effect of the arabinose and theophylline inducers (**Fig. 3A-B**). Importantly, this effect was extremely rapid (within minutes) and occurred in single cells prior to cell division (**Fig. 3, S2**). This makes it unlikely that PilT is indirectly promoting biogenesis through regulation of T4aP machine assembly, because the structural elements of the T4aP machine are likely inserted into the cell envelope through cell growth and division [43]. Indeed, a fluorescent fusion to MshJ, a component of the MSHA T4aP machine, demonstrated that the number of MSHA machines was similar in the parent and Δ*pilT* backgrounds (**Fig. S3**). Because ectopic expression of *pilT* in these experiments stimulated MSHA biogenesis, these data also further confirm that Δ*pilT* cells are not simply unpiliated due to runaway extension. Together, these data suggest that in addition to its defined role in promoting MSHA retraction, PilT also counterintuitively participates in the biogenesis of MSHA pili.

Some T4aP pili can undergo motor-independent retraction via the spontaneous depolymerization of the pilus filament [44]. Therefore, there are at least two distinct mechanisms by which PilT could support MSHA biogenesis. PilT can either (1) help promote MSHA pilus assembly, or (2) it can help maintain extended MSHA pili on the surface. If PilT is needed to maintain extended MSHA pili, we hypothesized that depleting PilT protein from piliated cells should result in the rapid loss of surface pili due to the subsequent motor-independent retraction of pili. The rapid depletion of PilT was accomplished by adapting a previously described orthogonal degron system from *Mesoplasma florum* [45, 46]. The translational fusion of a degron tag (called pdt2) to the C-terminus of native PilT (*i.e.*, PilT-pdt2) allows for the specific and temporally regulated degradation of PilT by induction of the cognate *M. florum* Lon protease (mf-Lon). Importantly, strains with *pilT*-pdt2 exhibited parental levels of piliation without mf-Lon expression and these pili still retracted, indicating that this fusion protein was functional (**Fig. S4A-C**). Pilus counts in strains with untagged PilT did not change upon mf-Lon induction, indicating that this protease does not pleiotropically affect MSHA piliation. The PilT-pdt2 strain also showed no change in piliation upon induction of the mf-Lon protease (**Fig. S4A-B**), which suggested that the loss of PilT did not result in the loss of surface pili via motor-independent retraction. To confirm that PilT-pdt2 was actually degraded in these experiments, we also measured PilT-dependent retraction following depletion. The PilT-pdt2 strain exhibited reduced pilus retraction only when mf-Lon was induced (**Fig. S4C**), which indicates that these cells were depleted of PilT activity as expected. Together, these data indicate that MSHA pili do not exhibit spontaneous retraction in the absence of PilT. Thus, PilT is not required to maintain extended pili, but instead helps to promote MSHA pilus biogenesis. Because Δ*pilT* cells occasionally generate a single long pilus, this also suggests that PilT is not required for processive pilus extension, but is instead likely required for initiating pilus extension.

187 Because PilT promotes both MSHA extension and retraction, we next wanted to
188 investigate whether both activities relied on motor-dependent ATPase activity. In addition to
189 PilT, *V. cholerae* also expresses PilU, a PilT-dependent accessory retraction motor ATPase.
190 Loss of PilU alone (Δ*pilU*) did not impact MSHA pilus biogenesis, and the loss of PilU did not
191 further exacerbate the piliation defect of the Δ*pilT* mutant (Δ*pilTU*) (**Fig. 4A-B**). PilU is incapable
192 of mediating retraction in the absence of PilT, but it can promote retraction in the presence of an
193 ATPase defective allele of PilT [25, 47]. To test if PilTU-dependent MSHA retraction and
194 extension were linked, we also assessed piliation in the ATPase defective Walker A mutant of
195 PilT ($pilT^{K136A}$). Although this allele is ATPase-defective, retraction can still occur in this
196 background through the ATPase-activity of PilU (**Fig. 4C**). While the retraction-capable $pilT^{K136A}$
197 mutant exhibited parental levels of MSHA piliation, the retraction-deficient $pilT^{K136A}$ Δ*pilU* mutant
198 exhibited a loss of MSHA piliation (**Fig. 4A-C**). Together, these data indicate that the ATPase-
199 dependent activity required for MSHA retraction is also needed for initiating MSHA pilus
200 extension.
201 Our data thus far are consistent with a model wherein PilT helps initiate MSHA
202 extension. The MshE extension motor is also required for MSHA biogenesis and extension.
203 Thus, we hypothesized that if PilT helps initiate MSHA extension, it may directly interact with the
204 MshE extension motor to carry out this activity. By contrast, since PilT is not required for
205 extension of competence pili, we hypothesized that PilT may not directly interact with the
206 competence pilus extension motor PilB. Because our data suggest that PilU can promote MSHA
207 extension in the $pilT^{K136A}$ background, we also wanted to assess whether this accessory
208 retraction ATPase could directly interact with the extension motors. To assess interactions
209 between these motors, we carried out bacterial adenylate cyclase two-hybrid (BACTH) analysis
210 of the retraction motors (PilT and PilU) with the MSHA extension motor MshE and the
211 competence pilus extension motor PilB. Interactions of the retraction motors with the MSHA
212 platform protein (MshG) were also included as a positive control. The BACTH analysis showed
213 that the retraction motors (PilT and PilU) do interact with MshE (**Fig. S5**), which was consistent
214 with our hypothesis. However, these BACTH assays also showed interactions between the
215 retraction motors and PilB (**Fig. S5**). Since the retraction motors interacted with both MshE and
216 PilB, the physiological relevance for these interactions is unclear. PilB does not require PilTU
217 activity to extend the competence pilus, so the direct interaction between the motors tested in
218 this assay may not be indicative of a functional interaction.
219 To better understand the factors that regulate MSHA pilus extension, we also took an
220 unbiased genetic approach. The presence of multiple surface pili is required for optimal MSHA-
221 dependent attachment to surfaces [48]. Therefore, we took advantage of the poor attachment of
222 Δ*pilT* cells to the walls of plastic culture tubes to select for suppressor mutants with improved
223 binding. We hypothesized that this would occur through the restoration of MSHA surface
224 piliation. Through this genetic selection, we isolated 14 suppressor mutants that exhibited
225 parental levels of binding and restored MSHA piliation. Whole genome resequencing revealed
226 that all of the suppressor mutants had point mutations in the *mshA* major pilin, with 6 distinct
227 *mshA* suppressor alleles identified (**Fig. S6A**). These suppressor mutations predominantly
228 clustered around the predicted kink within the N-terminal α-helix (**Fig. 5A**). We reconstructed
229 each of these mutations in clean genetic backgrounds, which revealed that all of these *mshA*
230 alleles increased MSHA piliation in the Δ*pilT* background (**Fig. 5B-C**). Correspondingly, these
231 mutations also restored surface attachment to parental levels (**Fig. S6B**). Western blot analysis
232 indicated that these alleles did not increase piliation by increasing the expression of the major
233 pilin (**Fig. 5B**). Furthermore, all of these suppressor *mshA* mutants could still retract in the

234 presence of PilT and lacked the ability to retract efficiently in the absence of PilT, just like the
235 *mshA*$^{WT}$ parent. Thus, these suppressor mutations specifically enhanced MSHA surface piliation
236 in the Δ*pilT* background without markedly altering MSHA piliation or retraction in the presence of
237 *pilT*.
238 Since our previous data suggest that PilT initiates MSHA pilus extension, we
239 hypothesized that the *mshA* suppressor mutants bypass the need for PilT by independently
240 promoting pilus extension. In canonical T4aP, minor pilins – proteins that structurally resemble
241 the major pilin but are expressed at significantly lower levels – form an initiation complex that
242 primes pilus assembly [49-51]. One possibility is that the MSHA T4aP system minor pilins are
243 not naturally capable of initiating pilus extension without the aid of PilT. If so, the suppressor
244 mutations in *mshA* could help enhance MSHA pilus extension in the absence of PilT akin to a
245 canonical T4aP minor pilin. As a result, we hypothesized that only low concentrations of the
246 mutated MshA suppressor allele would be required to initiate pilus extension. We chose
247 *mshA*$^{P31S}$ as a representative suppressor because it was centrally located among the other
248 suppressors, it was hit most frequently in the selection, and because we predicted that the
249 disruption of the proline might generate the strongest impact on the structure of the protein. To
250 test induction of low levels of *mshA*$^{P31S}$, we generated constructs that ectopically expressed
251 *mshA*$^{P31S}$ under the control of a tightly regulated $P_{tac}$-riboswitch promoter, in a background that
252 still expressed native *mshA* but lacked *pilT* (*i.e.*, $P_{tac}$-ribo-*mshA*$^{P31S}$ Δ*pilT*). If MshA$^{P31S}$ helps
253 initiate pilus extension like a minor pilin, we hypothesized that it should be able to recover
254 piliation even at low levels of induction. However, we found that full induction of the *mshA*$^{P31S}$
255 allele was required to increase pilus number (**Fig. S7A-B**). An equivalent construct inducing the
256 wild-type *mshA* allele showed no change in pilus number, indicating that the observed effect on
257 piliation requires ectopic expression of the *mshA*$^{P31S}$ suppressor allele. MshA expression from
258 the $P_{tac}$-riboswitch-*mshA* construct was assessed by Western blot analysis in a background that
259 lacked native *mshA* (**Fig. S7C**), which revealed that full induction resulted in native levels of
260 MshA expression (**Fig. S7C**). Furthermore, we found that ectopic *mshA* induction in the
261 presence of native *mshA* (*i.e.*, assessing MshA levels in the same strains used in **Fig. S7B**)
262 resulted in additive levels of MshA (**Fig. S7C**). These data suggest that the MshA suppressor
263 alleles do not initiate pilus extension at low levels (akin to a canonical T4aP minor pilin), but they
264 do not negate the hypothesis that these alleles help initiate pilus assembly, albeit inefficiently.
265 If MshA$^{P31S}$ helps initiate pilus extension in the absence of PilT, we hypothesized that the
266 expression of this allele should promote assembly of wildtype MshA major pilins co-expressed
267 in the same background. This cannot be distinguished in the experiments described above (**Fig.
268 S7A-C**) because both the native *mshA* allele and the ectopically expressed *mshA* allele
269 contained the T70C mutation required for fluorescent labeling. We therefore generated strains
270 where only the native or ectopically expressed *mshA* allele contained the T70C mutation so that
271 the assembly of each allele could be distinguished by fluorescently labeling cells with AF488-
272 mal. If MshA$^{P31S}$ can help initiate pilus assembly in the Δ*pilT* background, then we would expect
273 ectopic expression of MshA$^{P31S}$ (which cannot be labeled) to promote the assembly of natively
274 expressed MshA$^{T70C}$ (which can be labeled) into fluorescent pilus filaments. Conversely, if
275 MshA$^{P31S}$ does not help initiate pilus assembly and instead assembles into distinct filaments,
276 then no change in surface piliation should be observed when MshA$^{P31S}$ is induced. When we
277 performed this experiment, we found that surface piliation was recovered following induction of
278 MshA$^{P31S}$ (native *mshA*$^{T70C}$ + ectopic *mshA*$^{P31S}$) to a level that resembled the scenarios when
279 MshA$^{P31S}$ could be fluorescently labeled (native *mshA*$^{WT}$ + ectopic *mshA*$^{P31S,T70C}$; native
280 *mshA*$^{T70C}$ + ectopic *mshA*$^{P31S,T70C}$) (**Fig. S7D**). Importantly, ectopic overexpression of *mshA*

281 alleles that lacked the P31S mutation (native *mshA*$^{WT}$ + ectopic *mshA*$^{T70C}$; native *mshA*$^{T70C}$ +
282 ectopic *mshA*$^{WT}$) did not restore surface piliation (**Fig. 7D**). Together, these data indicate that
283 *mshA*$^{P31S}$ does promote the assembly of *mshA*$^{WT}$ into pilus filaments, which is consistent with a
284 model wherein this *mshA* suppressor allele helps initiate pilus assembly.
285
286 **DISCUSSION**
287 Here, we have explored the mechanistic basis for PilT-dependent MSHA piliation in *V. cholerae*.
288 We demonstrate that PilT is not needed to disrupt runaway extension or maintain pili in their
289 extended state. Instead, our data are consistent with a model in which PilT counterintuitively
290 promotes MSHA pilus extension in addition to its established role in pilus retraction. The
291 strongest evidence for this model comes from the observation that the temporally controlled
292 ectopic expression of *pilT* in Δ*pilT* cells results in the rapid extension of MSHA pili (**Fig. 3, S2**).
293 Furthermore, we show that both PilT-dependent extension and retraction rely on the ATPase
294 activity of the retraction motor, which can be accomplished by PilT alone, or by the presence of
295 PilU when PilT ATPase activity is disrupted. Because we could not recover MSHA piliation by
296 altering the activity and/or expression level of the MshE extension motor, it is tempting to
297 speculate that PilT and MshE interact to coordinately promote pilus extension (**Fig. 6**). However,
298 the exact mechanism underlying PilT-dependent extension of MSHA pili remains unclear. It is
299 possible that PilT promotes the interaction of MshE with the pilus machine *in vivo* to facilitate
300 extension or that the interaction between MshE and PilT stimulates MshE ATPase activity.
301 Exploring these questions will be the focus of future work.
302 Our results suggest that MSHA pilus biogenesis and dynamics are not the result of direct
303 competition between the extension and retraction motors in *V. cholerae*. Instead, it is the
304 combined activities of these motors that allow pilus extension to take place. Recent work
305 highlights that distinct motor ATPases can coordinate to promote pilus extension and/or
306 retraction. As discussed above, PilU is an accessory retraction motor that works in conjunction
307 with PilT to promote retraction of T4aP [15, 25]. In *Acinetobacter baylyi*, optimal T4aP extension
308 depends on the combined activity of two distinct extension motors, TfpB and PilB, where TfpB
309 initiates pilus extension and PilB promotes processive extension [14]. MSHA extension may be
310 similarly regulated, through the cooperative activities of an extension and retraction motor (*i.e.*,
311 MshE and PilT). PilT, however, is also clearly required for MSHA retraction. This bidirectional
312 activity resembles *Caulobacter crescentus* CpaF, which is the sole motor ATPase expressed in
313 this T4cP tad pilus system, and powers both pilus extension and retraction [52]. Indeed, recent
314 structural analysis of the transitions adopted by PilT suggest that this family of ATPase motors
315 may be able to adopt distinct configurations that can switch the directionality of their activity
316 (from retraction to extension) [53].
317 Our suppressor screen also implicated the structure of the major pilin in regulating
318 MSHA biogenesis (**Fig. 5**). Most of the suppressor mutations obtained were localized near a
319 proline in the widely conserved N-terminal α-helix of T4aP major pilins that is also known as the
320 α1 subdomain [54]. This proline introduces a kink into α1 [55], and is hypothesized to affect the
321 packing of major pilin subunits within the filament. Indeed, mutations near the conserved proline
322 in the major pilin of the *Myxococcus xanthus* T4aP have been shown to impact pilus assembly
323 and/or retraction [56]. Because our data indicate that PilT likely promotes initiation of MSHA
324 pilus extension, we hypothesize that these MshA suppressor alleles also enhance initiation of
325 pilus extension to allow for pilus biogenesis in the absence of PilT (**Fig. 6**). This is supported by
326 the observation that the MshA$^{P31S}$ suppressor allele can promote assembly of the MshA$^{parent}$
327 major pilin into a pilus filament. Additionally, we have recently shown that the packing of major

328 pilin subunits within the pilus filament plays an important role in regulating motor-independent
329 retraction of T4aP [44]. This suggests that the major pilin and the structure of the pilus filament
330 are factors that likely contribute to the regulation of both T4aP extension and retraction.
331 Ultimately, this study describes two unappreciated factors that influence pilus extension
332 of the *V. cholerae* MSHA pili: the PilT retraction motor and the structure of the MSHA major
333 pilin. Because PilT is also required for piliation in other T4aP systems [57, 58], it is likely that the
334 mechanisms described here are not limited to the MSHA pili of *V. cholerae*. Also, recent
335 phylogenetic analysis indicates that MSHA pilus systems form a discrete cluster from canonical
336 T4aP [1]. Thus, it is tempting to speculate that PilT-dependent extension may be a conserved
337 property among this subcategory of T4P. More broadly, these results help expand our
338 understanding of the factors that regulate the biogenesis and dynamic activity of these nearly
339 ubiquitous bacterial surface appendages.
340
341 **METHODS**
342 *Bacterial strains and culture conditions*
343 *Vibrio cholerae* E7946 was used as the background for all strains employed in this study.
344 Cultures were grown in LB broth (Miller) and plated on LB agar, and incubations were carried
345 out at 30°C. Descriptions of all strains used in this study are found in **Supplemental Table 1**.
346 Where appropriate, media were supplemented with kanamycin 50 µg/mL, trimethoprim 10
347 µg/mL, spectinomycin 200 µg/mL, chloramphenicol 1 µg/mL, carbenicillin 100 µg/mL, or zeocin
348 100 µg/mL.
349
350 *Construction of mutant strains*
351 Splicing-by-overlap extension PCR was used to generate mutant constructs, as described
352 previously [59]. Natural transformation and cotransformation were used to introduce mutant
353 constructs into chitin-induced competent *V. cholerae* as described previously [60, 61]. Mutations
354 were confirmed by PCR and/or sequencing. All ectopic expression constructs were derived from
355 previously published strains [42]. The primers used to generate mutant constructs can be found
356 in **Supplemental Table 2**.
357
358 *Microscopy and image analysis*
359 All phase contrast and fluorescence images were obtained with a Nikon Ti-2 microscope with a
360 Plan Apo 60X objective, GFP filter cube, Hamamatsu ORCAFlash 4.0 camera, and Nikon NIS
361 Elements imaging software. Images were prepared with Fiji [62, 63].
362
363 Pili were visualized by Alexa Fluor 488-maleimide (AF488-mal) labelling. Cells were grown in LB
364 to an $OD_{600}$ of ~0.5 at 30°C rolling, with the exception of samples for imaging competence pili
365 (which were grown in LB + 100 µM IPTG + 20 mM $MgCl_2$ + 10 mM $CaCl_2$ to an $OD_{600}$ of ~2.5) or
366 samples imaging *mshJ-mCherry* (which were grown in LB overnight). Cells were then washed
367 and resuspended in instant ocean medium (7 g/L; Aquarium Systems) and incubated with 25
368 µg/mL AF488-mal for 10 min at room temperature. Cells were washed twice to remove excess
369 dye and resuspended in instant ocean medium. After labelling, cells were loaded on a glass
370 coverslip, covered with a 0.2% gelzan pad, and imaged. Lookup tables were chosen to best
371 represent piliation for each image unless otherwise noted. Pilus number was assessed by
372 randomly selecting 100 cells in a field of view in the phase channel for each replicate and then
373 manually scoring piliation in each cell. The percent of piliated cells that exhibited retraction was
374 assessed for each replicate by randomly selecting ~25 piliated cells and then observing

retraction during a 3-minute timelapse (frames taken with 100ms exposure every 3 sec). The retraction of any pili within a cell was used as a positive indicator of retraction. Three biological replicates were included for each dataset.

To quantify cell body fluorescence, cells were labelled and imaged as described above, with the exception that cells were incubated with AF488-mal for 30 min. Cell body detection and fluorescence quantification on regions containing ~300 total cells was carried out using MicrobeJ [64]. Data sets were manually curated to remove piliated cells, overlapping cells, and dead cells. Three biological replicates were included for each dataset.

*Temporally regulated induction of pilT*

Cells were first labelled, added to a coverslip, and covered with an 0.2% gelzan pad as described above. For **Fig. S2**, to observe how quickly cells could respond to inducer, cells were imaged under pads that either contained or lacked the inducers: 1.5 mM theophylline + 0.15% arabinose. An image was taken immediately upon exposure to the gelzan pad, and again after 15 min incubation at room temperature. For a more quantitative comparison of piliation following induction as shown in **Fig. 3**, cells were first loaded under a gelzan pad containing no inducer and allowed to recover for 5 min. A second 0.2% gelzan pad containing 3 mM theophylline + 0.4% arabinose was then layered on top of the first gelzan pad. The use of stacked gelzan pads in this experiment allowed for the slower diffusion of inducer molecules to cells (*i.e.*, via the diffusion of inducers through the gelzan pad in immediate contact with the cells). This ensured that any change in piliation was due to the effect of the inducer rather than recovery from conditions experienced during labeling and setup. Cells were imaged immediately ("- inducer") and then again after 45 min, which we empirically determined was sufficient for the inducer to diffuse into the lower pad ("+ inducer"). Piliation states were quantified as above, for each of the three biological replicates.

*Degradation of pilT*

Strains were labelled as described above and then allowed to incubate for 2.5 hrs with either inducer (0.2% arabinose) or vector control (an equivalent volume of water) to induce mf-Lon. Cells were then loaded onto a coverslip, covered with an 0.2% gelzan pad, and imaged as described above. Piliation state was scored as described above. Retraction was scored over a 3 min timelapse as described above, but categorized into either "no retraction", "some retraction", or "all pili retract". This was to reflect the more subtle effects seen during PilT depletion compared to when *pilT* is deleted.

*Western blotting*

Cells were grown to an $OD_{600}$ of ~0.5 at 30°C rolling. To assess cell associated MshA, cells were spun down (~1.5 x $10^9$ CFUs) and resuspended in an equivalent volume of instant ocean medium (*i.e.*, cells only). To assess the amount of MshA that was cell associated and shed, an aliquot of culture was used directly for Western blot analysis (*i.e.*, cells + sup). Samples were mixed 1:1 with 2 x SDS sample buffer [200 mM Tris pH 6.8, 25% glycerol, 1.8% SDS, 0.02% Bromophenol Blue, 5% β-mercaptoethanol] and then incubated at 95°C for 10 min, separated by SDS PAGE (15% gel), and then electrophoretically transferred to a PVDF membrane. This membrane was blocked with 5% milk and then incubated simultaneously with rabbit polyclonal α-MshA (1:1000, gift of J. Zhu) and mouse monoclonal α-RpoA (1:1000, Biolegend) (as a loading control) primary antibodies. Blots were washed and then incubated simultaneously with

α-mouse and α-rabbit secondary antibodies conjugated to horseradish peroxidase enzyme. Blots were developed with Pierce™ ECL Western Blotting Substrate and then imaged with a ProteinSimple FluorChem R system.

*Bacterial adenylate cyclase two-hybrid assay*

Genes of interest were amplified via PCR and cloned into the BACTH vectors pKT25 and pUT18C to produce N-terminal fusions between the target protein and the T25 and T18 fragments of adenylate cyclase, respectively. Miniprepped plasmids (Qiagen) were then co-transformed into *E. coli* BTH101 cells. As a positive control, T25-zip and T18-zip vectors were cotransformed into BTH101. As a negative control, the pKT25 and pUT18C empty vectors were cotransformed into BTH101. Transformations were plated onto LB + kanamycin (50 µg/mL) + carbenicillin (100 µg/mL) plates to select for transformants that received both plasmids. These transformants were then picked and grown overnight at 30°C in LB + kanamycin (50 µg/mL) + carbenicillin (100 µg/mL). Finally, 3 µL of the overnight cultures were spotted onto LB agar plates supplemented with 500 µM IPTG, kanamycin (50 µg/mL), carbenicillin (100 µg/mL), and X-gal (40 µg/mL). These plates were allowed to incubate statically at 30 °C for ~ 24 hours prior to imaging on an Epson Perfection V600 photo flatbed scanner.

*Genetic suppressor selection*

20 independent cultures of Δ*pilT* Δ*vps* were started from ~100 CFUs to generate independent lineages for this suppressor screen. Cells were grown in polystyrene culture tubes to an $OD_{600}$ of ~1.5 at 30°C rolling. A small aliquot was removed from each culture tube to be used for quantitative plating on LB agar (total cells). Tubes were then dumped and rinsed 5 times with fresh LB to remove unbound cells. Bound cells were then removed from the walls of the culture tube by adding 3 mL of fresh LB medium and vortexing vigorously for 30 sec. The cell slurry was then centrifuged, concentrated, and subjected to quantitative plating on LB agar (bound cells). The binding frequency was calculated for each sample by dividing the CFU after rinsing (bound cells) by the CFU before rinsing (total cells). Cells retrieved after binding were used to inoculate the next round of selection. Recursive rounds of selection were continued for each lineage until the binding frequency was at least 100x higher than the parental Δ*pilT* Δ*vps* control (4-8 rounds selection). Genomic DNA from select clones was used to generate sequencing libraries by homopolymer tail mediated ligation PCR (HTML-PCR) exactly as previously described [65] and then sequenced on an Illumina Next-Seq instrument. The resulting sequencing data was mapped to the N16961 genome [66] using CLC Genomics WorkBench and the Basic Variant Analysis tool was used to identify SNVs.

*Binding assays*

Cells were grown to an $OD_{600}$ of ~2.5 at 30°C shaking and 4 mL of culture was loaded into a new polystyrene culture tube. Tubes were incubated on a roller drum at room temperature for 20 min, during which time cells were allowed to bind to the walls of the tube. After incubation, a small aliquot was removed from each culture tube to be used for quantitative plating on LB agar (total cells). Then, tubes were dumped and rinsed 5 times with fresh LB to remove unbound cells. Bound cells were then removed from the walls of the culture tube by adding 1 mL of fresh LB medium and vortexing vigorously for 30 sec. The cell slurry was then centrifuged, concentrated, and subjected to quantitative plating on LB agar (bound cells). The binding frequency was calculated for each sample by dividing the CFU after rinsing (bound cells) by the CFU before rinsing (total cells). Three biological replicates were carried out for each strain.

## ACKNOWLEDGEMENTS

We would like to thank Clay Fuqua, Julia van Kessel, and Tuli Mukhophadyay for helpful discussions. We would also like to thank Jay Zhu for providing α-MshA antibody. This work was supported by grant R35GM128674 (to ABD).

## AUTHOR CONTRIBUTIONS

H. Hughes, C. Ellison, and A. Dalia conceptualized the experiments. Investigation was carried out by H. Hughes and T. Dalia. H. Hughes and A. Dalia wrote the paper and incorporated feedback from all authors.

## REFERENCES

1. Denise R, Abby SS, Rocha EPC. Diversification of the type IV filament superfamily into machines for adhesion, protein secretion, DNA uptake, and motility. PLOS Biology. 2019;17(7):e3000390-e. doi: 10.1371/journal.pbio.3000390.
2. Merz AJ, So M, Sheetz MP. Pilus retraction powers bacterial twitching motility. Nature. 2000;407(6800):98-102. Epub 2000/09/19. doi: 10.1038/35024105. PubMed PMID: 10993081.
3. O'Toole GA, Kolter R. Flagellar and twitching motility are necessary for *Pseudomonas aeruginosa* biofilm development. Molecular Microbiology. 1998;30(2):295-304.
4. Ellison CK, Dalia TN, Vidal Ceballos A, Wang JC-Y, Biais N, Brun YV, et al. Retraction of DNA-bound type IV competence pili initiates DNA uptake during natural transformation in Vibrio cholerae. Nature Microbiology. 2018;3(7):773-80. doi: 10.1038/s41564-018-0174-y.
5. Seitz P, Blokesch M. DNA-uptake machinery of naturally competent Vibrio cholerae. Proceedings of the National Academy of Sciences of the United States of America. 2013;110(44):17987-92. doi: 10.1073/pnas.1315647110.
6. Berne C, Ellison CK, Ducret A, Brun YV. Bacterial adhesion at the single-cell level. Nature Reviews Microbiology. 2018;16(10):616-27. doi: 10.1038/s41579-018-0057-5.
7. Ellison CK, Kan J, Dillard RS, Kysela DT, Ducret A, Berne C, et al. Obstruction of pilus retraction stimulates bacterial surface sensing. Science. 2017;358(6362):535-8. doi: 10.1126/science.aan5706. PubMed PMID: 29074778.
8. Watnick PI, Kolter R. Steps in the development of a Vibrio cholerae El Tor biofilm. Molecular microbiology. 1999;34(3):586-95.
9. Imhaus A-F, Duménil G. The number of Neisseria meningitidis type IV pili determines host cell interaction. The EMBO Journal. 2014;33(16):1767-83. doi: 10.1093/emboj/19.23.6408.
10. McCallum M, Tammam S, Khan A, Burrows LL, Howell PL. The molecular mechanism of the type IVa pilus motors. Nature Communications. 2017;8:15091-. doi: 10.1038/ncomms15091.
11. Koch MD, Fei C, Wingreen NS, Shaevitz JW, Gitai Z. Competitive binding of independent extension and retraction motors explains the quantitative dynamics of type IV pili. Proc Natl Acad Sci U S A. 2021;118(8). Epub 2021/02/18. doi: 10.1073/pnas.2014926118. PubMed PMID: 33593905; PubMed Central PMCID: PMCPMC7923367.
12. Chang YW, Rettberg LA, Treuner-Lange A, Iwasa J, Sogaard-Andersen L, Jensen GJ. Architecture of the type IVa pilus machine. Science. 2016;351(6278):aad2001. Epub 2016/03/12. doi: 10.1126/science.aad2001. PubMed PMID: 26965631; PubMed Central PMCID: PMCPMC5929464.
13. Aubey F, Corre JP, Kong Y, Xu X, Obino D, Goussard S, et al. Inhibitors of the Neisseria meningitidis PilF ATPase provoke type IV pilus disassembly. Proc Natl Acad Sci U S A. 2019;116(17):8481-6. Epub 2019/04/06. doi: 10.1073/pnas.1817757116. PubMed PMID: 30948644; PubMed Central PMCID: PMCPMC6486710.

14. Ellison CK, Dalia TN, Klancher CA, Shaevitz JW, Gitai Z, Dalia AB. Acinetobacter baylyi regulates type IV pilus synthesis by employing two extension motors and a motor protein inhibitor. Nat Commun. 2021;12(1):3744. Epub 2021/06/20. doi: 10.1038/s41467-021-24124-6. PubMed PMID: 34145281; PubMed Central PMCID: PMCPMC8213720.

15. Chlebek JL, Hughes HQ, Ratkiewicz AS, Rayyan R, Wang JC, Herrin BE, et al. PilT and PilU are homohexameric ATPases that coordinate to retract type IVa pili. PLoS Genet. 2019;15(10):e1008448. Epub 2019/10/19. doi: 10.1371/journal.pgen.1008448. PubMed PMID: 31626631; PubMed Central PMCID: PMCPMC6821130.

16. Wolfgang M, van Putten JP, Hayes SF, Dorward D, Koomey M. Components and dynamics of fiber formation define a ubiquitous biogenesis pathway for bacterial pili. EMBO J. 2000;19(23):6408-18. Epub 2000/12/02. doi: 10.1093/emboj/19.23.6408. PubMed PMID: 11101514; PubMed Central PMCID: PMCPMC305860.

17. Whitchurch CB, Mattick JS. Characterization of a gene, pilU, required for twitching motility but not phage sensitivity in Pseudomonas aeruginosa. Molecular Microbiology. 1994;13(6):1079-91. doi: 10.1111/j.1365-2958.1994.tb00499.x.

18. Wolfgang M, Lauer P, Park HS, Brossay L, Hebert J, Koomey M. PilT mutations lead to simultaneous defects in competence for natural transformation and twitching motility in piliated *Neisseria gonorrhoeae*. Mol Microbiol. 1998;29(1):321-30. Epub 1998/08/14. doi: 10.1046/j.1365-2958.1998.00935.x. PubMed PMID: 9701824.

19. Morand PC, Bille E, Morelle S, Eugè Ne E, Beretti J-L, Wolfgang M, et al. Type IV pilus retraction in pathogenic Neisseria is regulated by the PilC proteins. The EMBO Journal. 2004;23:2009-17. doi: 10.1038/sj.emboj.7600200.

20. Chakraborty S, Monfett M, Maier TM, Benach JL, Frank DW, Thanassi DG. Type IV pili in Francisella tularensis: roles of pilF and pilT in fiber assembly, host cell adherence, and virulence. Infect Immun. 2008;76(7):2852-61. Epub 2008/04/23. doi: 10.1128/IAI.01726-07. PubMed PMID: 18426883; PubMed Central PMCID: PMCPMC2446743.

21. Varga JJ, Nguyen V, O'Brien DK, Rodgers K, Walker RA, Melville SB. Type IV pili-dependent gliding motility in the Gram-positive pathogen Clostridium perfringens and other Clostridia. Mol Microbiol. 2006;62(3):680-94. Epub 2006/09/27. doi: 10.1111/j.1365-2958.2006.05414.x. PubMed PMID: 16999833.

22. Floyd KA, Lee CK, Xian W, Nametalla M, Valentine A, Crair B, et al. c-di-GMP modulates type IV MSHA pilus retraction and surface attachment in Vibrio cholerae. Nat Commun. 2020;11(1):1549. Epub 2020/03/28. doi: 10.1038/s41467-020-15331-8. PubMed PMID: 32214098; PubMed Central PMCID: PMCPMC7096442.

23. Hughes HQ, Floyd KA, Hossain S, Anantharaman S, Kysela DT, Zöldi M, et al. Nitric oxide stimulates type IV MSHA pilus retraction in Vibrio cholerae via activation of the phosphodiesterase CdpA. Proceedings of the National Academy of Sciences. 2022;119(7). doi: 10.1073/pnas.2108349119.

24. Jones CJ, Utada A, Davis KR, Thongsomboon W, Zamorano Sanchez D, Banakar V, et al. C-di-GMP Regulates Motile to Sessile Transition by Modulating MshA Pili Biogenesis and Near-Surface Motility Behavior in Vibrio cholerae. PLOS Pathogens. 2015;11(10):e1005068-e. doi: 10.1371/journal.ppat.1005068.

25. Adams DW, Pereira JM, Stoudmann C, Stutzmann S, Blokesch M. The type IV pilus protein PilU functions as a PilT-dependent retraction ATPase. PLoS Genet. 2019;15(9):e1008393. Epub 2019/09/17. doi: 10.1371/journal.pgen.1008393. PubMed PMID: 31525185; PubMed Central PMCID: PMCPMC6762196.

26. Ellison CK, Dalia TN, Dalia AB, Brun YV. Real-time microscopy and physical perturbation of bacterial pili using maleimide-conjugated molecules. Nat Protoc. 2019;14(6):1803-19. Epub 2019/04/28. doi: 10.1038/s41596-019-0162-6. PubMed PMID: 31028374; PubMed Central PMCID: PMCPMC7461830.

564 27. Hughes HQ, Floyd KA, Hossain S, Anantharaman S, Kysela DT, Zoldi M, et al. Nitric oxide
565 stimulates type IV MSHA pilus retraction in Vibrio cholerae via activation of the phosphodiesterase
566 CdpA. Proc Natl Acad Sci U S A. 2022;119(7). Epub 2022/02/10. doi: 10.1073/pnas.2108349119. PubMed
567 PMID: 35135874.
568 28. Chiavelli DA, Marsh JW, Taylor RK. The Mannose-Sensitive Hemagglutinin of Vibrio cholerae
569 Promotes Adherence to Zooplankton. Applied and environmental microbiology. 2001;67(7):3220-5. doi:
570 10.1128/aem.67.7.3220-3225.2001.
571 29. List C, Grutsch A, Radler C, Cakar F, Zingl FG, Schild-Prüfert K, et al. Genes Activated by Vibrio
572 cholerae upon Exposure to Caenorhabditis elegans Reveal the Mannose-Sensitive Hemagglutinin To Be
573 Essential for Colonization. mSphere. 2018;3(3). doi: 10.1128/mSphereDirect.00238-18.
574 30. Meibom KL, Li XB, Nielsen AT, Wu C-Y, Roseman S, Schoolnik GK. The Vibrio cholerae chitin
575 utilization program. 2004.
576 31. Ellison CK, Dalia TN, Vidal Ceballos A, Wang JC, Biais N, Brun YV, et al. Retraction of DNA-bound
577 type IV competence pili initiates DNA uptake during natural transformation in Vibrio cholerae. Nat
578 Microbiol. 2018;3(7):773-80. doi: 10.1038/s41564-018-0174-y. PubMed PMID: 29891864.
579 32. Seitz P, Blokesch M. DNA-uptake machinery of naturally competent Vibrio cholerae. Proc Natl
580 Acad Sci U S A. 2013;110(44):17987-92. Epub 2013/10/16. doi: 1315647110 [pii]

581 10.1073/pnas.1315647110. PubMed PMID: 24127573.
582 33. Wu SS, Wu J, Kaiser D. The Myxococcus xanthus pilT locus is required for social gliding motility
583 although pili are still produced. Mol Microbiol. 1997;23(1):109-21. Epub 1997/01/01. doi:
584 10.1046/j.1365-2958.1997.1791550.x. PubMed PMID: 9004225.
585 34. Comolli JC, Hauser AR, Waite L, Whitchurch CB, Mattick JS, Engel JN. Pseudomonas aeruginosa
586 gene products PilT and PilU are required for cytotoxicity in vitro and virulence in a mouse model of acute
587 pneumonia. Infect Immun. 1999;67(7):3625-30. Epub 1999/06/22. doi: 10.1128/IAI.67.7.3625-
588 3630.1999. PubMed PMID: 10377148; PubMed Central PMCID: PMCPMC116553.
589 35. Pujol C, Eugene E, Marceau M, Nassif X. The meningococcal PilT protein is required for induction
590 of intimate attachment to epithelial cells following pilus-mediated adhesion. Proc Natl Acad Sci U S A.
591 1999;96(7):4017-22. PubMed PMID: 10097155; PubMed Central PMCID: PMCPMC22412.
592 36. Bieber D, Ramer SW, Wu CY, Murray WJ, Tobe T, Fernandez R, et al. Type IV pili, transient
593 bacterial aggregates, and virulence of enteropathogenic Escherichia coli. Science. 1998;280(5372):2114-
594 8. PubMed PMID: 9641917.
595 37. Wu SS, Kaiser D. Regulation of expression of the pilA gene in Myxococcus xanthus. J Bacteriol.
596 1997;179(24):7748-58. Epub 1997/12/24. doi: 10.1128/jb.179.24.7748-7758.1997. PubMed PMID:
597 9401034; PubMed Central PMCID: PMCPMC179738.
598 38. Hobbs M, Collie ES, Free PD, Livingston SP, Mattick JS. PilS and PilR, a two-component
599 transcriptional regulatory system controlling expression of type 4 fimbriae in Pseudomonas aeruginosa.
600 Mol Microbiol. 1993;7(5):669-82. Epub 1993/03/01. doi: 10.1111/j.1365-2958.1993.tb01158.x. PubMed
601 PMID: 8097014.
602 39. Wang Y-C, Chin K-H, Tu Z-L, He J, Jones CJ, Sanchez DZ, et al. Nucleotide binding by the
603 widespread high-affinity cyclic di-GMP receptor MshEN domain. Nature Communications.
604 2016;7(1):12481-. doi: 10.1038/ncomms12481.
605 40. Nakhamchik A, Wilde C, Rowe-Magnus DA. Cyclic-di-GMP regulates extracellular polysaccharide
606 production, biofilm formation, and rugose colony development by Vibrio vulnificus. Appl Environ
607 Microbiol. 2008;74(13):4199-209. Epub 2008/05/20. doi: 10.1128/AEM.00176-08. PubMed PMID:
608 18487410; PubMed Central PMCID: PMCPMC2446529.
609 41. Fong JC, Yildiz FH. The rbmBCDEF gene cluster modulates development of rugose colony
610 morphology and biofilm formation in Vibrio cholerae. J Bacteriol. 2007;189(6):2319-30. Epub

611 2007/01/16. doi: 10.1128/JB.01569-06. PubMed PMID: 17220218; PubMed Central PMCID:
612 PMCPMC1899372.
613 42. Dalia TN, Chlebek JL, Dalia AB. A modular chromosomally integrated toolkit for ectopic gene
614 expression in Vibrio cholerae. Sci Rep. 2020;10(1):15398. Epub 2020/09/23. doi: 10.1038/s41598-020-
615 72387-8. PubMed PMID: 32958839; PubMed Central PMCID: PMCPMC7505983.
616 43. Carter T, Buensuceso RN, Tammam S, Lamers RP, Harvey H, Howell PL, et al. The Type IVa Pilus
617 Machinery Is Recruited to Sites of Future Cell Division. mBio. 2017;8(1). Epub 2017/02/02. doi:
618 10.1128/mBio.02103-16. PubMed PMID: 28143978; PubMed Central PMCID: PMCPMC5285504.
619 44. Chlebek JL, Denise R, Craig L, Dalia AB. Motor-independent retraction of type IV pili is governed
620 by an inherent property of the pilus filament. Proc Natl Acad Sci U S A. 2021;118(47). Epub 2021/11/19.
621 doi: 10.1073/pnas.2102780118. PubMed PMID: 34789573; PubMed Central PMCID: PMCPMC8617508.
622 45. Cameron DE, Collins JJ. Tunable protein degradation in bacteria. Nat Biotechnol.
623 2014;32(12):1276-81. Epub 2014/11/18. doi: 10.1038/nbt.3053. PubMed PMID: 25402616; PubMed
624 Central PMCID: PMCPMC4262603.
625 46. Chlebek JL, Dalia TN, Biais N, Dalia AB. Fresh Extension of Vibrio cholerae Competence Type IV
626 Pili Predisposes Them for Motor-Independent Retraction. Appl Environ Microbiol.
627 2021;87(14):e0047821. Epub 2021/05/16. doi: 10.1128/AEM.00478-21. PubMed PMID: 33990308;
628 PubMed Central PMCID: PMCPMC8231728.
629 47. Chlebek JL, Hughes HQ, Ratkiewicz AS, Rayyan R, Wang JC-Y, Herrin BE, et al. PilT and PilU are
630 homohexameric ATPases that coordinate to retract type IVa pili. PLOS Genetics. 2019;15(10):e1008448-
631 e. doi: 10.1371/journal.pgen.1008448.
632 48. Zhang W, Luo M, Feng C, Liu H, Zhang H, Bennett RR, et al. Crash landing of Vibrio cholerae by
633 MSHA pili-assisted braking and anchoring in a viscoelastic environment. eLife. 2021;10. Epub
634 2021/07/03. doi: 10.7554/eLife.60655. PubMed PMID: 34212857; PubMed Central PMCID:
635 PMCPMC8282333.
636 49. Ng D, Harn T, Altindal T, Kolappan S, Marles JM, Lala R, et al. The Vibrio cholerae Minor Pilin
637 TcpB Initiates Assembly and Retraction of the Toxin-Coregulated Pilus. PLoS Pathog.
638 2016;12(12):e1006109. Epub 2016/12/20. doi: 10.1371/journal.ppat.1006109. PubMed PMID:
639 27992883; PubMed Central PMCID: PMCPMC5207764.
640 50. Nguyen Y, Sugiman-Marangos S, Harvey H, Bell SD, Charlton CL, Junop MS, et al. Pseudomonas
641 aeruginosa minor pilins prime type IVa pilus assembly and promote surface display of the PilY1 adhesin.
642 J Biol Chem. 2015;290(1):601-11. Epub 2014/11/13. doi: 10.1074/jbc.M114.616904. PubMed PMID:
643 25389296; PubMed Central PMCID: PMCPMC4281761.
644 51. Treuner-Lange A, Chang YW, Glatter T, Herfurth M, Lindow S, Chreifi G, et al. PilY1 and minor
645 pilins form a complex priming the type IVa pilus in Myxococcus xanthus. Nat Commun. 2020;11(1):5054.
646 Epub 2020/10/09. doi: 10.1038/s41467-020-18803-z. PubMed PMID: 33028835; PubMed Central
647 PMCID: PMCPMC7541494.
648 52. Ellison CK, Kan J, Chlebek JL, Hummels KR, Panis G, Viollier PH, et al. A bifunctional ATPase drives
649 tad pilus extension and retraction. Sci Adv. 2019;5(12):eaay2591. Epub 2020/01/04. doi:
650 10.1126/sciadv.aay2591. PubMed PMID: 31897429; PubMed Central PMCID: PMCPMC6920026.
651 53. McCallum M, Benlekbir S, Nguyen S, Tammam S, Rubinstein JL, Burrows LL, et al. Multiple
652 conformations facilitate PilT function in the type IV pilus. Nat Commun. 2019;10(1):5198. Epub
653 2019/11/16. doi: 10.1038/s41467-019-13070-z. PubMed PMID: 31729381; PubMed Central PMCID:
654 PMCPMC6858323.
655 54. Craig L, Pique ME, Tainer JA. Type IV pilus structure and bacterial pathogenicity. Nature Reviews
656 Microbiology. 2004;2(5):363-78. doi: 10.1038/nrmicro885.

657 55. Craig L, Volkmann N, Arvai AS, Pique ME, Yeager M, Egelman EH, et al. Type IV pilus structure by
658 cryo-electron microscopy and crystallography: implications for pilus assembly and functions. Mol Cell.
659 2006;23(5):651-62. Epub 2006/09/05. doi: 10.1016/j.molcel.2006.07.004. PubMed PMID: 16949362.
660 56. Yang Z, Hu W, Chen K, Wang J, Lux R, Zhou ZH, et al. Alanine 32 in PilA is important for PilA
661 stability and type IV pili function in Myxococcus xanthus. Microbiology (Reading, England). 2011;157(Pt
662 7):1920-8. doi: 10.1099/mic.0.049684-0.
663 57. Chakraborty S, Monfett M, Maier TM, Benach JL, Frank DW, Thanassi DG. Type IV pili in
664 Francisella tularensis: roles of pilF and pilT in fiber assembly, host cell adherence, and virulence.
665 Infection and immunity. 2008;76(7):2852-61. doi: 10.1128/IAI.01726-07.
666 58. Varga JJ, Nguyen V, O'Brien DK, Rodgers K, Walker RA, Melville SB. Type IV pili-dependent gliding
667 motility in the Gram-positive pathogen Clostridium perfringens and other Clostridia. Molecular
668 Microbiology. 2006;62(3):680-94. doi: 10.1111/j.1365-2958.2006.05414.x.
669 59. Dalia AB, Lazinski DW, Camilli A. Characterization of undermethylated sites in Vibrio cholerae. J
670 Bacteriol. 2013;195(10):2389-99. Epub 2013/03/19. doi: 10.1128/JB.02112-12. PubMed PMID:
671 23504020; PubMed Central PMCID: PMCPMC3650525.
672 60. Dalia AB, McDonough E, Camilli A. Multiplex genome editing by natural transformation. Proc
673 Natl Acad Sci U S A. 2014;111(24):8937-42. Epub 2014/06/04. doi: 10.1073/pnas.1406478111. PubMed
674 PMID: 24889608; PubMed Central PMCID: PMCPMC4066482.
675 61. Dalia AB. Natural Cotransformation and Multiplex Genome Editing by Natural Transformation
676 (MuGENT) of Vibrio cholerae. Methods Mol Biol. 2018;1839:53-64. Epub 2018/07/27. doi: 10.1007/978-
677 1-4939-8685-9_6. PubMed PMID: 30047054.
678 62. Rueden CT, Schindelin J, Hiner MC, DeZonia BE, Walter AE, Arena ET, et al. ImageJ2: ImageJ for
679 the next generation of scientific image data. BMC Bioinformatics. 2017;18(1):529. Epub 2017/12/01. doi:
680 10.1186/s12859-017-1934-z. PubMed PMID: 29187165; PubMed Central PMCID: PMCPMC5708080.
681 63. Schindelin J, Arganda-Carreras I, Frise E, Kaynig V, Longair M, Pietzsch T, et al. Fiji: an open-
682 source platform for biological-image analysis. Nature Methods. 2012;9(7):676-82. doi:
683 10.1038/nmeth.2019.
684 64. Ducret A, Quardokus EM, Brun YV. MicrobeJ, a tool for high throughput bacterial cell detection
685 and quantitative analysis. Nat Microbiol. 2016;1(7):16077. Epub 2016/08/31. doi:
686 10.1038/nmicrobiol.2016.77. PubMed PMID: 27572972; PubMed Central PMCID: PMCPMC5010025.
687 65. Lazinski DW, Camilli A. Homopolymer tail-mediated ligation PCR: a streamlined and highly
688 efficient method for DNA cloning and library construction. Biotechniques. 2013;54(1):25-34. Epub
689 2013/01/15. doi: 000113981 [pii]

690 10.2144/000113981. PubMed PMID: 23311318.
691 66. Heidelberg JF, Eisen JA, Nelson WC, Clayton RA, Gwinn ML, Dodson RJ, et al. DNA sequence of
692 both chromosomes of the cholera pathogen Vibrio cholerae. Nature. 2000;406(6795):477-83. doi:
693 10.1038/35020000. PubMed PMID: 10952301.
694 67. Jumper J, Evans R, Pritzel A, Green T, Figurnov M, Ronneberger O, et al. Highly accurate protein
695 structure prediction with AlphaFold. Nature. 2021;596(7873):583-9. Epub 2021/07/16. doi:
696 10.1038/s41586-021-03819-2. PubMed PMID: 34265844; PubMed Central PMCID: PMCPMC8371605.
697 68. Miller VL, DiRita VJ, Mekalanos JJ. Identification of toxS, a regulatory gene whose product
698 enhances toxR-mediated activation of the cholera toxin promoter. J Bacteriol. 1989;171(3):1288-93.
699 Epub 1989/03/01. doi: 10.1128/jb.171.3.1288-1293.1989. PubMed PMID: 2646275; PubMed Central
700 PMCID: PMCPMC209743.

701
702
703

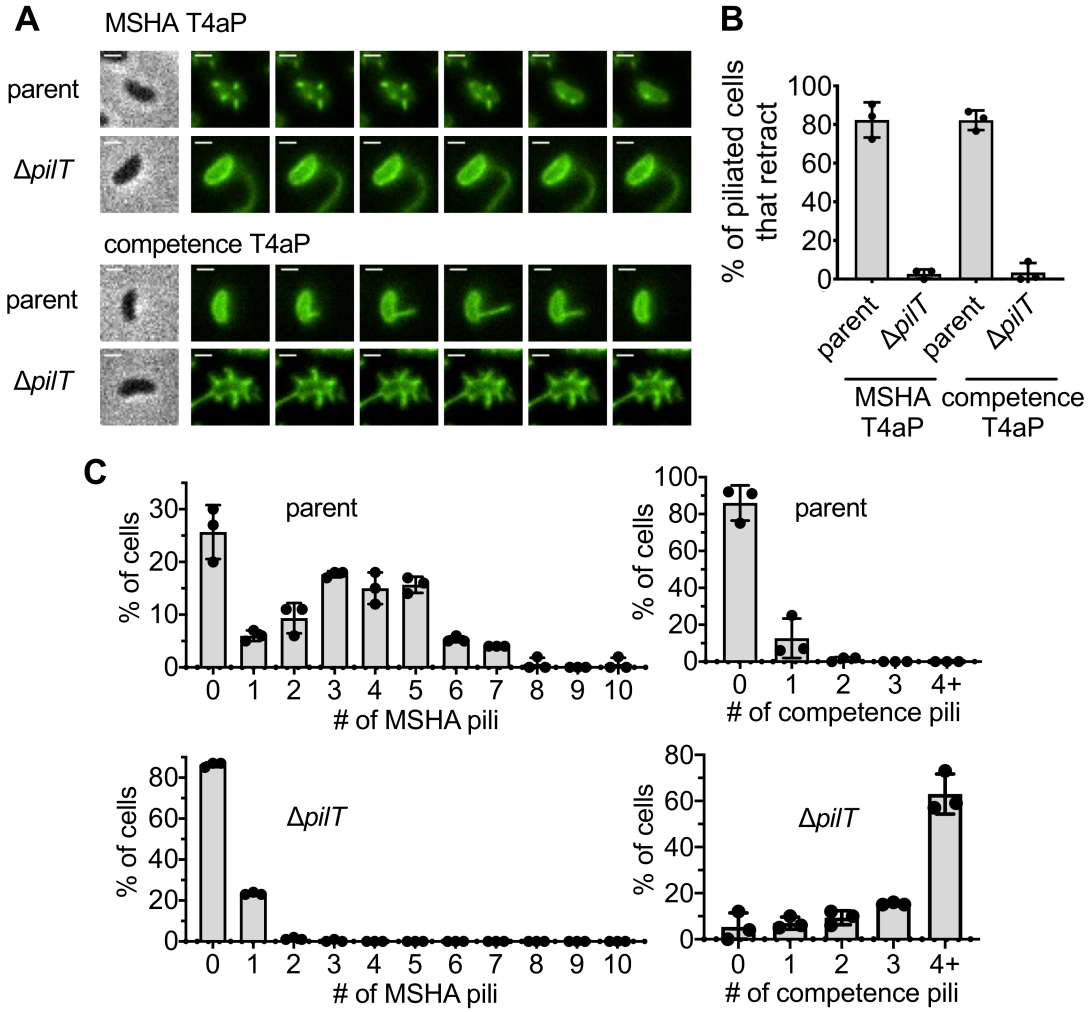


**Fig. 1. PilT has a distinct impact on *V. cholerae* MSHA and competence T4aP surface piliation**. (**A**) Representative montage of piliated AF488-mal labeled cells for the pilus system indicated. Strains contain either *mshA*$^{T70C}$ (to label MSHA pili) or *pilA*$^{S67C}$ (to label competence pili). Phase images (left) are included from the first frame of the montage and show the cell boundary. Fluorescent images show AF488-mal labeled pili and there are 6-s intervals between frames. Scale bar = 1 µm. (**B**) Quantification of MSHA or competence T4aP retraction. Graph displays the percentage of piliated cells in each replicate that exhibited any pilus retraction during a three-minute timelapse. $n \geq 25$ piliated cells analyzed for each of the three biological replicates. (**C**) Quantification of MSHA and competence pili in parent and Δ*pilT* cells as indicated. $n = 300$ cells analyzed from three independent biological replicates for all samples. All data are displayed as the mean ± SD.

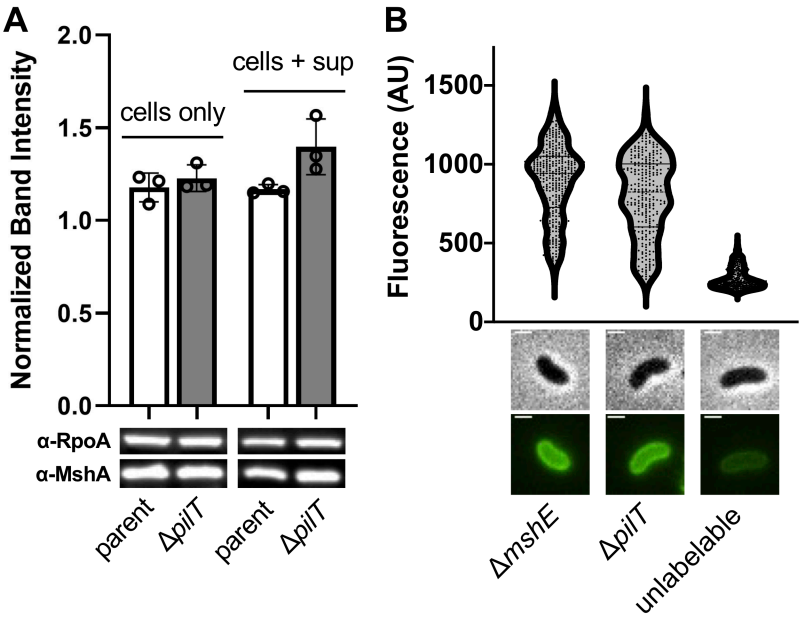


**Fig. 2. Reduced MSHA piliation of Δ*pilT* cells is likely due to a lack of pilus biogenesis rather than "runaway" extension.** (A) Western blot analysis of MshA protein levels in parent and Δ*pilT* strains. Samples represent either cell-associated major pilin (cells only) or cell associated + pili shed in the supernatant (cells + sup). Band intensities are normalized to the RpoA loading control for quantification. Data are from three independent biological replicates. (B) Quantification of cell body fluorescence in AF488-maleimide labeled cells as indicated. The Δ*mshE* and Δ*pilT* strains contain the *mshA*$^{T70C}$ mutation required for labeling the major pilin, while the unlabelable strain lacks this mutation. The latter is included here to denote the background cell body fluorescence observed in the absence of major pilins that can be labeled. Only unpiliated cells were analyzed, and $n \geq 275$ cells from three independent biological replicates for each strain. Representative images of cells used for quantification are included below. Phase images show cell boundaries and fluorescence images show AF488-mal labeled cells. Lookup tables are equivalent between fluorescence images. Scale bar = 1 μm.

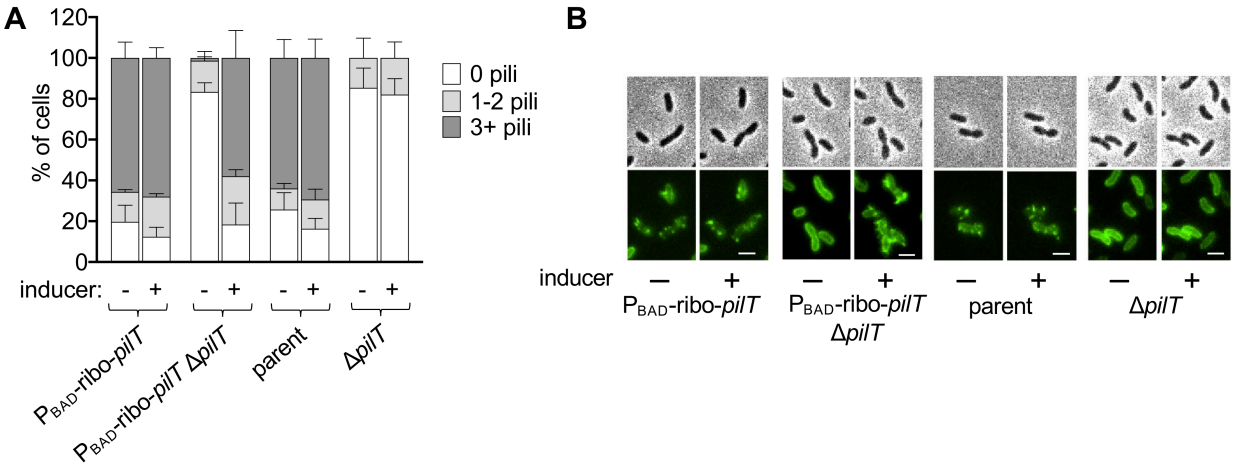


**Fig. 3. PilT promotes MSHA pilus extension**. (**A**) Quantification of piliation in strains imaged before and after induction with 0.2% arabinose + 1.5 mM theophylline. Cells were categorized as either having no pili (white bars), 1-2 pili (light gray bars), or at least 3 pili (dark gray bars). *n* = 300 cells analyzed from three independent biological replicates for all samples and data are displayed as the mean ± SD. (**B**) Representative images of cells from strains in **A**. Phase images (top) show cell boundaries and fluorescence images (bottom) show AF488-mal labeled pili. Each sample is shown before ("−") and after ("+") induction. Scale bar = 2 μm.

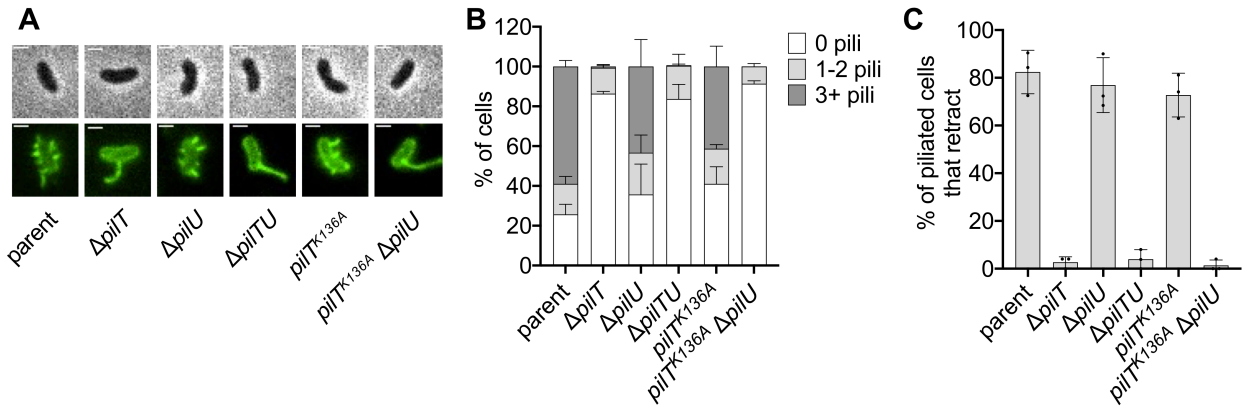


741
742
743 **Fig. 4. Retraction motor ATPase activity is required for MSHA surface piliation**. (**A**) Representative
744 images of piliated cells containing the indicated mutations to their retraction motor ATPases. Phase
745 images (top) show cell boundaries and fluorescence images (bottom) show AF488-mal labeled pili. Scale
746 bar = 1 µm. (**B**) Quantification of piliation in strains from **A**. Cells were categorized as either having no pili
747 (white bars), 1-2 pili (light gray bars), or at least 3 pili (dark gray bars). *n* = 300 cells analyzed from three
748 independent biological replicates for all samples. Data for the parent and Δ*pilT* strains are identical to that
749 presented in **Fig. 1C** and are included again here for ease of comparison. (**C**) Quantification of retraction
750 in strains from **A**. Graphs display the percentage of cells in each replicate that exhibited any pilus
751 retraction during a three-minute timelapse. *n* ≥ 25 piliated cells analyzed for each of the three biological
752 replicates. All data are displayed as the mean ± SD. Parent and Δ*pilT* data from **Fig 1A** are included for
753 comparison.
754

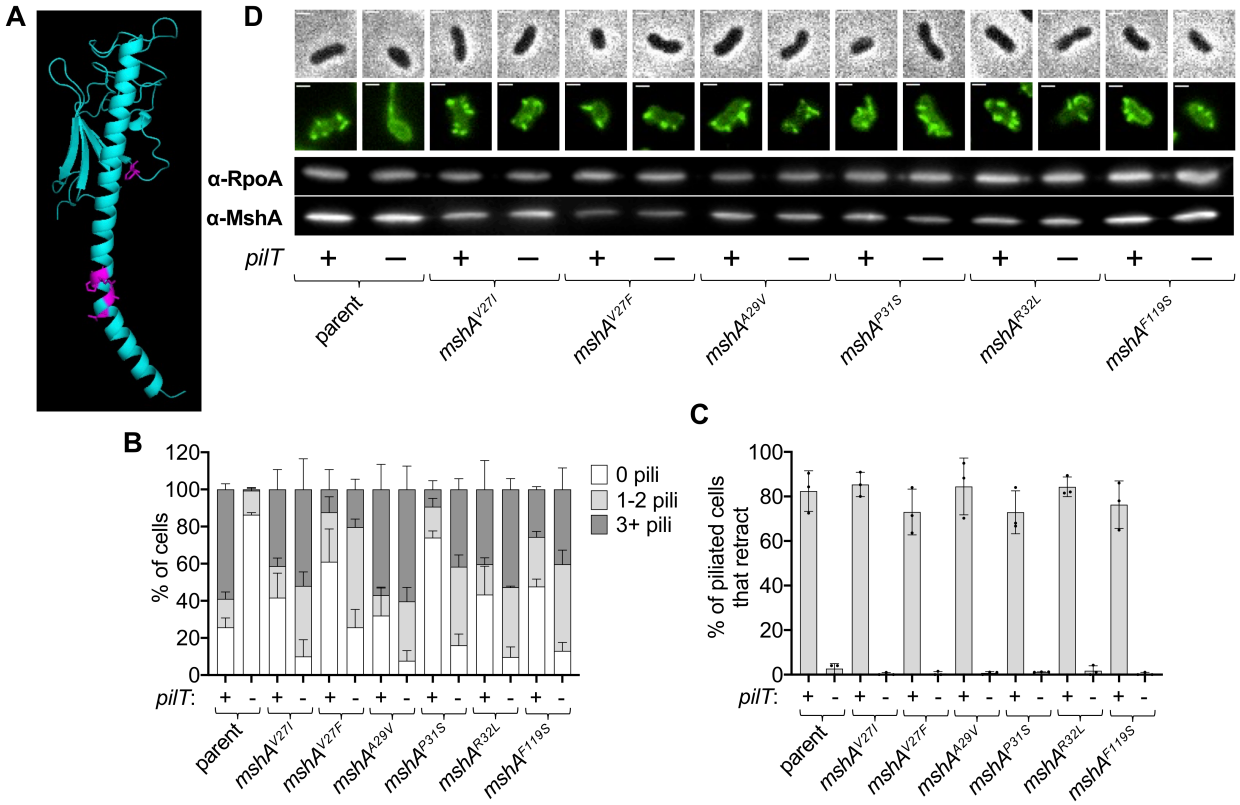


**Fig. 5. Point mutations in the major pilin *mshA* recover the piliation defect of a Δ*pilT* mutant**. (**A**) Predicted structure of MshA, generated using Alphafold [67]. Residues mutated in the suppressor selection are colored magenta. (**B**) Quantification of piliation in strains harboring the indicated *mshA* alleles. Cells were categorized as either having no pili (white bars), 1-2 pili (light gray bars), or at least 3 pili (dark gray bars). *n* = 300 cells analyzed from three independent biological replicates for all samples. (**C**) Quantification of retraction in strains harboring the indicated *mshA* alleles. Data displays the percentage of cells in each replicate that exhibited any pilus retraction during a three-minute timelapse. *n* ≥ 25 piliated cells analyzed for each of the three biological replicates. Data in **B** and **C** are shown as the mean ± SD. Data for the parent and Δ*pilT* strains are identical to that presented in **Fig. 1C** and are included again here for ease of comparison. (**D**) Representative images of piliated cells and Western blotting of MshA in strains from **B** and **C**. RpoA is included as a loading control. Phase images (top) show cell boundaries and fluorescence images (below) show AF488-mal labeled pili. Scale bar = 1 μm. In all panels, strains that retain native *pilT* are denoted "+" and strains with Δ*pilT* mutations are denoted "–".

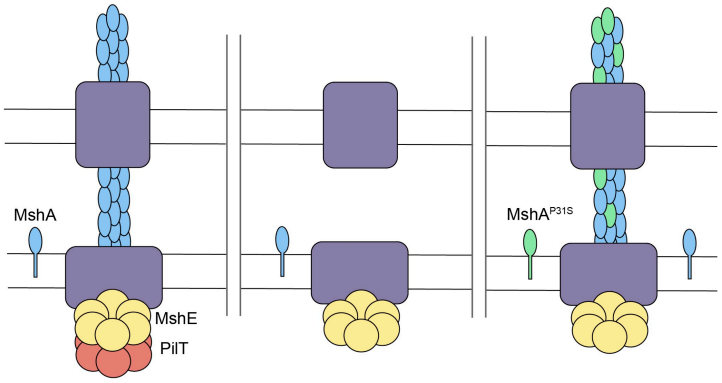


**Fig. 6. Model for the proposed mechanisms that promote MSHA extension and surface piliation**. In wildtype cells (left), MshE and PilT are both required to promote extension of MshA into a pilus filament. In the absence of PilT (middle), pili do not extend and surface piliation is dramatically reduced. Mutations in the MshA major pilin, such as MshA$^{P31S}$, (right) can promote MSHA pilus assembly in the absence of PilT.

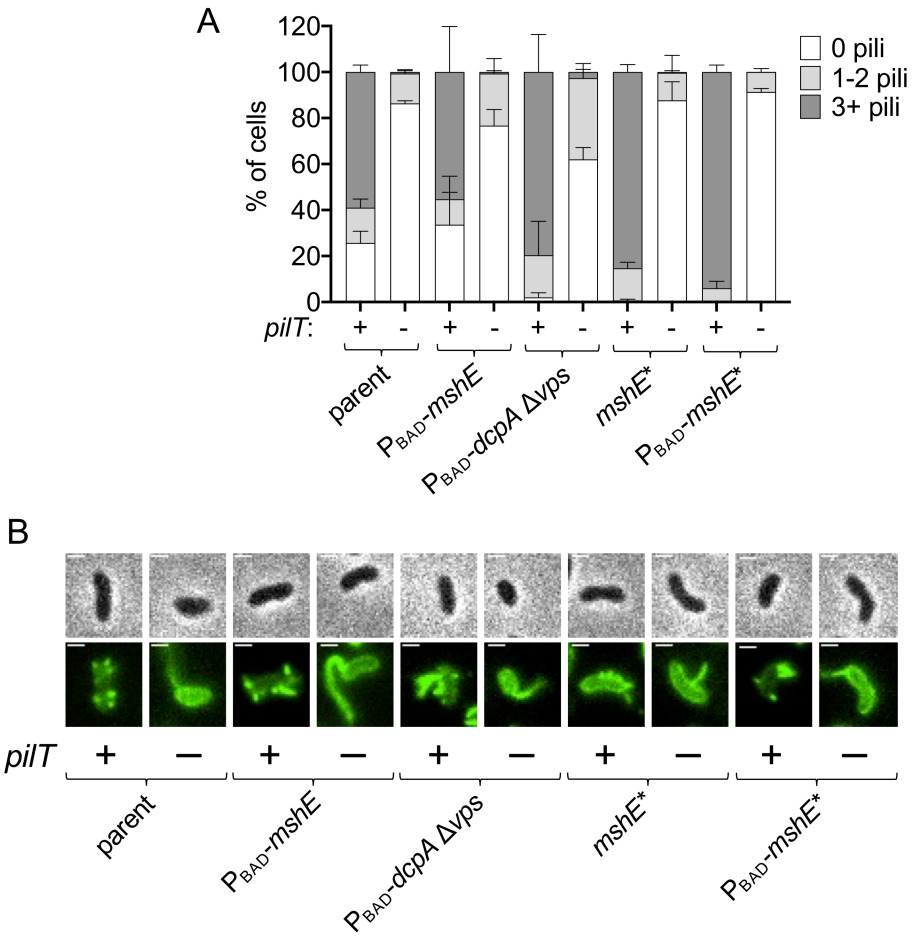


**Fig. S1. The piliation defect in the Δ*pilT* mutant cannot be recovered by increasing MshE expression or activity.** (**A**) Quantification of piliation in strains with altered extension motor regulation. Strains that retain native *pilT* are denoted "+" and strains with Δ*pilT* mutations are denoted "−". Cells were categorized as either having no pili (white bars), 1-2 pili (light gray bars), or at least 3 pili (dark gray bars). *n* = 300 cells analyzed from three independent biological replicates for all samples and data are displayed as the mean ± SD. All strains with ectopic $P_{BAD}$ constructs were induced with 0.2% arabinose. Data for the parent and Δ*pilT* strains are identical to that presented in **Fig. 1C** and are included again here for ease of comparison. (**B**) Representative images of piliated cells from strains in **A**. Phase images (top) show cell boundaries and fluorescence images (bottom) show AF488-mal labeled pili. Strains that retain native *pilT* are denoted "+" and strains with Δ*pilT* mutations are denoted "−". Scale bar = 1 μm.

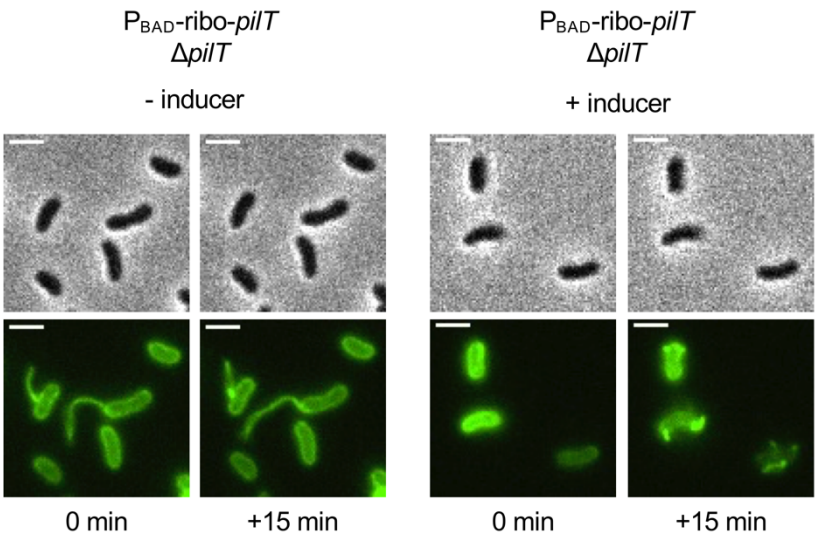


**Fig. S2. Induction of *pilT* rapidly recovers MSHA surface piliation.** Representative images of a $P_{BAD}$-ribo-*pilT ΔpilT* strain when *pilT* expression is rapidly induced under the microscope. Phase images (top) show cell boundaries and fluorescence images (bottom) show AF488-mal labeled pili. Samples were applied to a slide with a gelzan pad either lacking inducer (left; "- inducer") or including 0.2% arabinose and 1.5mM theophylline as an inducer ("+ inducer"). Each sample was imaged immediately after application of the gelzan pad ("0 min") and again after 15 min ("+15 min"). Scale bar = 2 μm.

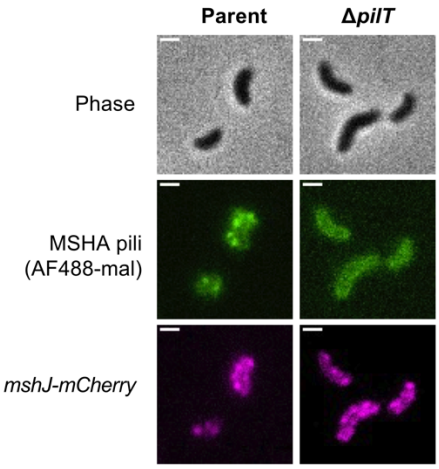


801
802
803 **Fig. S3. Loss of PilT does not affect the assembly of MSHA pilus machines**. Representative images
804 of parent and Δ*pilT* strains containing a functional MshJ-mCherry fusion to label MSHA T4P machines.
805 Phase images (top) show cell boundaries, green images (middle) show AF488-mal labeled pili, and red
806 images (bottom) show MshJ-mCherry localization. Strain that retains native *pilT* is denoted "+" and strain
807 with Δ*pilT* mutation is denoted "−". Scale bar = 2 μm.
808

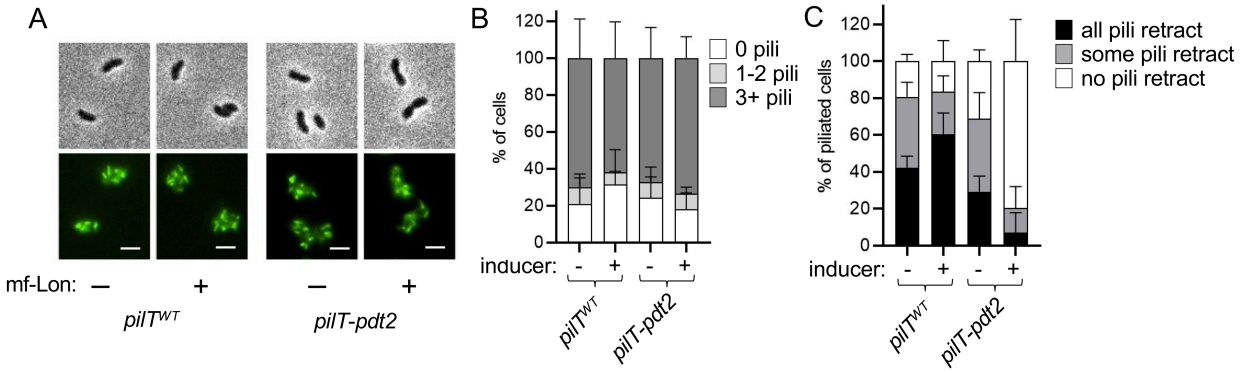


**Fig. S4. PilT is not required to maintain MSHA surface piliation**. (**A**) Representative images of cells where mf-Lon was ("+"; 0.2% arabinose) or was not ("-") induced. Phase images (top) show cell boundaries and fluorescence images (bottom) show AF488-mal labeled pili. Scale bar = 1 µm. (**B**) Quantification of piliation in samples from **A**. Cells were categorized as either having no pili (white bars), 1-2 pili (light gray bars), or at least 3 pili (dark gray bars). *n* = 300 cells analyzed from three independent biological replicates for all samples. (**C**) Quantification of retraction in samples from **A**. Graph displays the percentage of cells in each replicate that retracted all, some, or no pili during a three-minute timelapse. *n* ≥ 25 piliated cells analyzed for each of the three biological replicates. All data are displayed as the mean ± SD.

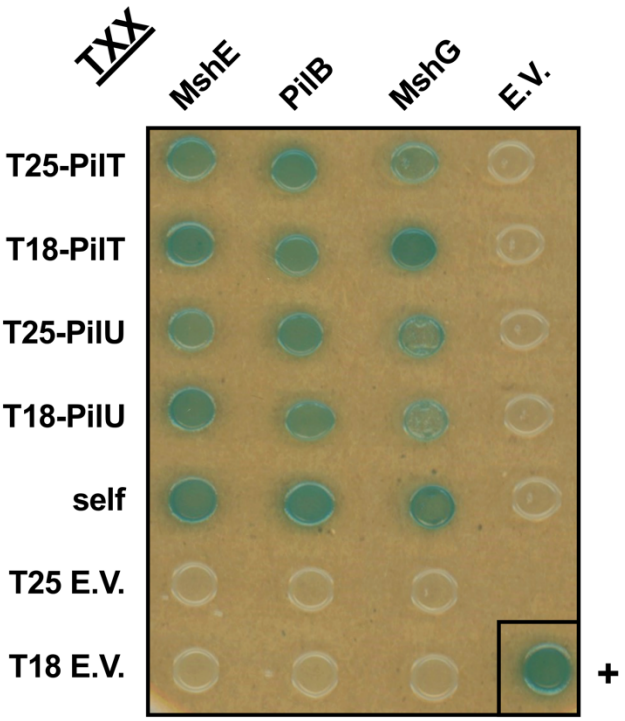


**Fig. S5. PilT and PilU directly interact with the MshE and PilB extension motors**. Representative image of a BACTH assay between T25- and T18- fusions of the indicated proteins. Both PilT and PilU displayed strong interactions with themselves ("self"), the extension motors (MshE and PilB), as well as the MSHA platform protein (MshG). "E.V." denotes a pairing with an empty vector, and "+" indicates the BACTH positive control (T25-Zip + T18-Zip). This image is representative of three independent experiments.

A

| Location in unprocessed pilin | Location in processed pilin | Number of independent hits |
|---|---|---|
| V27I | V18I | 2 |
| V27F | V18F | 3 |
| A29V | A20V | 1 |
| P31S | P22S | 5 |
| R32L | R23L | 2 |
| F119S | F110S | 1 |

B

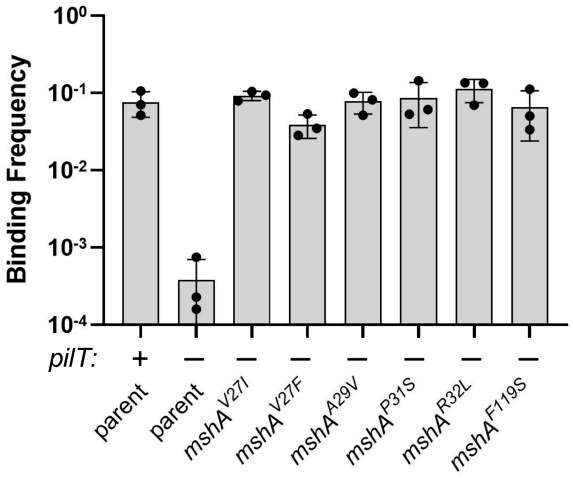


**Fig. S6. MshA suppressor mutants enhance adherence**. (**A**) Table of the MshA mutations isolated in the Δ*pilT* suppressor screen. The relative position of the mutated residues is indicated relative to the MshA start codon (Location in unprocessed pilin) and relative to the first amino acid in the pilin after being processed by the pre-pilin peptidase (Location in processed pilin). ”Number of independent hits” denotes the number of distinct genetic lines in which the indicated suppressor mutation was isolated. (**B**) Binding frequency of the indicated strains to the wall of culture tubes. Strains that retain native *pilT* are denoted “+” and strains with Δ*pilT* mutations are denoted “−”. Data are from three independent biological replicates and shown as the mean ± SD.

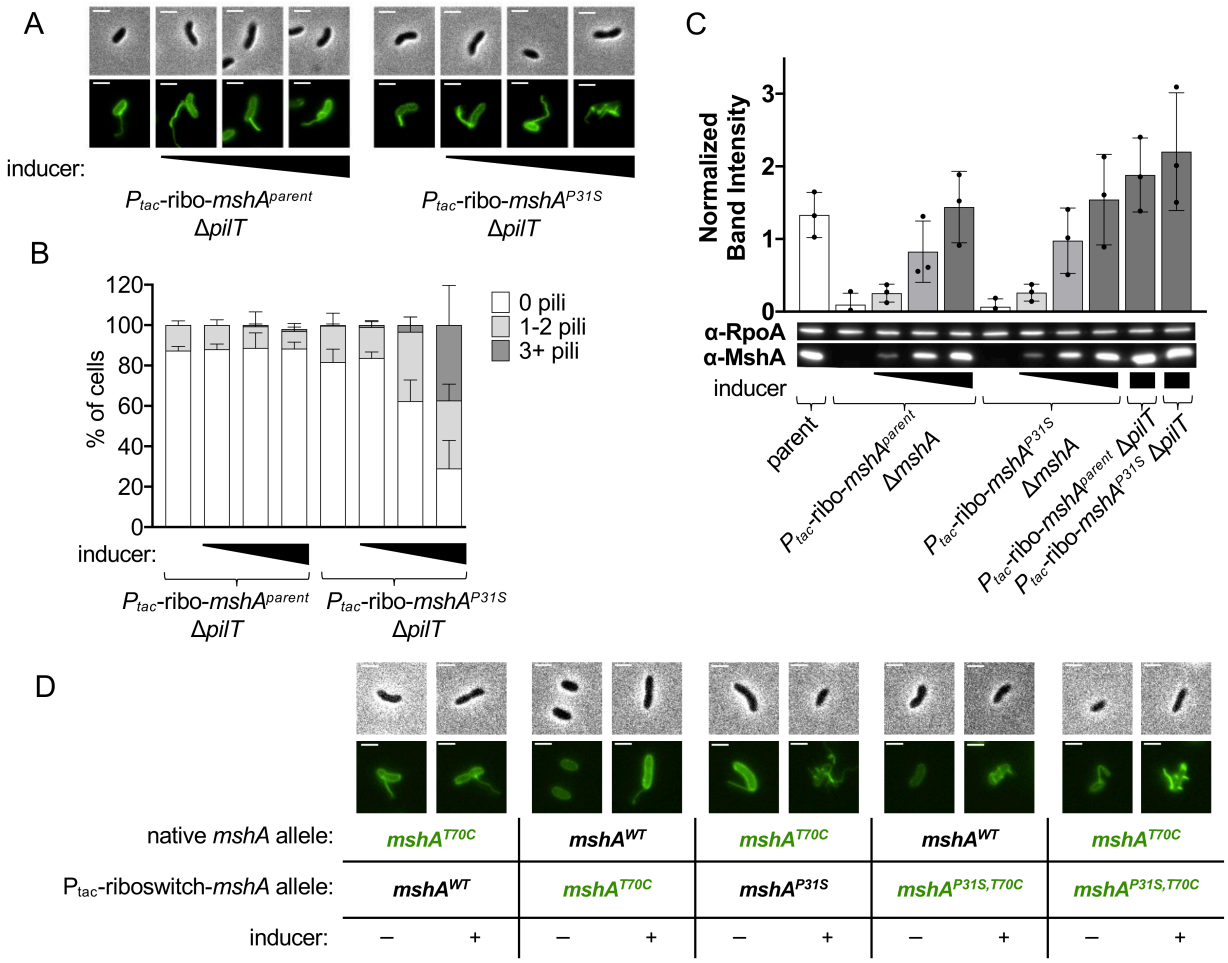


**Fig. S7. MshA$^{P31S}$ promotes assembly of native MshA in the absence of *pilT*.** (**A**) Representative images of piliated cells from strains under increasing induction of either $P_{tac}$-riboswitch-*mshA*$^{parent}$ or $P_{tac}$-riboswitch-*mshA*$^{P31S}$. All *mshA* alleles in these strains (native and ectopic) contain the T70C mutation needed for AF488-mal labeling. Concentrations of inducer used from left to right: (1) 0 μM IPTG + 0 μM theophylline, (2) 5 μM IPTG + 75 μM theophylline, (3) 20 μM IPTG + 300 μM theophylline, and (4) 100 μM IPTG + 1.5 mM theophylline. Phase images (top) show cell boundaries and fluorescence images (bottom) show AF488-mal labeled pili. Scale bar = 2 μm. (**B**) Quantification of piliation in samples from **A**. Cells were categorized as either having no pili (white bars), 1-2 pili (light gray bars), or at least 3 pili (dark gray bars). *n* = 300 cells analyzed from three independent biological replicates for all samples. (**C**) Western blot quantification of cell-associated MshA in the indicated strains in the induction conditions used in **A** and **B**. Band intensities are normalized to the RpoA loading control. Data are from three independent biological replicates. All data are displayed as the mean ± SD. (**D**) Representative images of cells from Δ*pilT* strains expressing the indicated *mshA* allele at the native locus (native *mshA* allele) and ectopic locus ($P_{tac}$-riboswitch-*mshA* allele). Cells were either grown with ("+") or without ("-") 100 μM IPTG + 1.5 mM theophylline to induce the ectopic $P_{tac}$-riboswitch-*mshA* allele in the strain as indicated. Only the alleles containing the T70C mutation can be labeled with AF488-mal and are denoted in green text in the table below the images. Lookup tables are equivalent between fluorescent images in **D** to accurately reflect the expression level of the labelable *mshA* allele. Scale bar = 2 μm.

862 **Table S1: Strain List**

| Strain name in manuscript | Figure | Genotype and antibiotic resistances | Strain # | Reference |
|---|---|---|---|---|
| parent (MSHA T4aP) | Fig. 1A, 1B, 1C, 2A, 3A, 3B, 4A, 4B, 4C, 5B, 5C, 5D, S1A, S1B, S6B, S7C | E7946 $Sm^R$, ΔVC1807::$Kan^R$, *mshA*$^{T70C}$ | CAH764 (SAD3125) | [22, 23] |
| Δ*pilT* (MSHA T4aP) | Fig. 1A, 1B, 1C, 2A, 2B, 3A, 3B, 4A, 4B, 4C, 5B, 5C, 5D, S1A, S1B, S6B | E7946 $Sm^R$, ΔVC1807::$Kan^R$, *mshA*$^{T70C}$, Δ*pilT*::$Tm^R$ | HKQ001 (SAD3144) | [22, 23] |
| Parent (competence T4aP) | Fig. 1A, 1B, 1C | E7946 $Sm^R$, ΔVC1807::$Zeo^R$, Δ*lacZ*::*lacIq*, $P_{tac}$-*tfoX*, Δ*luxO*::miniFRT, *pilA*$^{S56C}$ | TND0905 (SAD2468) | [15] |
| Δ*pilT* (competence T4aP) | Fig. 1A, 1B, 1C | E7946 $Sm^R$, ΔVC1807::$Zeo^R$, Δ*lacZ*::*lacIq*, $P_{tac}$-*tfoX*, Δ*luxO*::miniFRT, *pilA*$^{S56C}$, Δ*pilT*::$Tm^R$ | TND1035 (SAD2469) | [15] |
| Δ*mshE* | Fig. 2B | E7946 $Sm^R$, ΔVC1807::$Kan^R$, *mshA*$^{T70C}$, Δ*mshE*::miniFRT | TND0503 (SAD3198) | [23] |
| unlabelable | Fig. 2B | E7946 $Sm^R$ | SAD030 | [68] |
| $P_{BAD}$-ribo-*pilT* | Fig. 3A, 3B | E7946 $Sm^R$, ΔVC1807::$Kan^R$, *mshA*$^{T70C}$, ΔVCA0692::$P_{BAD}$-riboswitch-*pilT* $Carb^R$ | HKQ483 (SAD3303) | This study |
| $P_{BAD}$-ribo-*pilT* Δ*pilT* | Fig. 3A, 3B, S2 | E7946 $Sm^R$, ΔVC1807::$Kan^R$, *mshA*$^{T70C}$, ΔVCA0692::$P_{BAD}$-riboswitch-*pilT* $Carb^R$, Δ*pilT*::$Tm^R$ | HKQ484 (SAD3304) | This study |
| Δ*pilU* | Fig. 4A, 4B, 4C | E7946 $Sm^R$, ΔVC1807::$Cm^R$, *mshA*$^{T70C}$, Δ*pilU*::miniFRT | TND0471 (SAD3305) | This study |
| Δ*pilTU* | Fig. 4A, 4B, 4C | E7946 $Sm^R$, ΔVC1807::$Kan^R$, *mshA*$^{T70C}$, Δ*pilTU*::$Tm^R$ | JLC419 (SAD3306) | This study |
| *pilT*$^{K136A}$ | Fig. 4A, 4B, 4C | E7946 $Sm^R$, ΔVC1807::$Spec^R$, *mshA*$^{T70C}$, *pilT*$^{K136A}$ | HKQ006 (SAD3307) | This study |
| *pilT*$^{K136A}$ Δ*pilU* | Fig. 4A, 4B, 4C | E7946 $Sm^R$, ΔVC1807::$Kan^R$, *mshA*$^{T70C}$, *pilT*$^{K136A}$, Δ*pilU*::$Tm^R$ | JLC446 (SAD3308) | This study |
| *mshA*$^{V27I}$ | Fig. 5B, 5C, 5D | E7946 $Sm^R$, ΔVC1807::$Spec^R$, *mshA*$^{T70C, V27I}$ | HKQ025 (SAD3309) | This study |
| *mshA*$^{V27I}$ Δ*pilT* | Fig. 5B, 5C, 5D, S6B | E7946 $Sm^R$, ΔVC1807::$Spec^R$, *mshA*$^{T70C, V27I}$, Δ*pilT*::$Tm^R$ | HKQ031 (SAD3310) | This study |
| *mshA*$^{V27F}$ | Fig. 5B, 5C, 5D | E7946 $Sm^R$, ΔVC1807::$Spec^R$, *mshA*$^{T70C, V27F}$ | HKQ026 (SAD3311) | This study |
| *mshA*$^{V27F}$ Δ*pilT* | Fig. 5B, 5C, 5D, S6B | E7946 $Sm^R$, ΔVC1807::$Spec^R$, *mshA*$^{T70C, V27F}$, Δ*pilT*::$Tm^R$ | HKQ032 (SAD3312) | This study |
| *mshA*$^{A29V}$ | Fig. 5B, 5C, 5D | E7946 $Sm^R$, ΔVC1807::$Spec^R$, *mshA*$^{T70C, A29V}$ | HKQ027 (SAD3313) | This study |
| *mshA*$^{A29V}$ Δ*pilT* | Fig. 5B, 5C, 5D, S6B | E7946 $Sm^R$, ΔVC1807::$Spec^R$, *mshA*$^{T70C, A29V}$, Δ*pilT*::$Tm^R$ | HKQ033 (SAD3314) | This study |
| *mshA*$^{P31S}$ | Fig. 5B, 5C, 5D | E7946 $Sm^R$, ΔVC1807::$Spec^R$, *mshA*$^{T70C, P31S}$ | HKQ028 (SAD3315) | This study |
| *mshA*$^{P31S}$ Δ*pilT* | Fig. 5B, 5C, 5D, S6B | E7946 $Sm^R$, ΔVC1807::$Spec^R$, *mshA*$^{T70C, P31S}$, Δ*pilT*::$Tm^R$ | HKQ034 (SAD3316) | This study |
| *mshA*$^{R32L}$ | Fig. 5B, 5C, 5D | E7946 $Sm^R$, ΔVC1807::$Spec^R$, *mshA*$^{T70C, R32L}$ | HKQ029 (SAD3317) | This study |
| *mshA*$^{R32L}$ Δ*pilT* | Fig. 5B, 5C, 5D, S6B | E7946 $Sm^R$, ΔVC1807::$Spec^R$, *mshA*$^{T70C, R32L}$, Δ*pilT*::$Tm^R$ | HKQ035 (SAD3318) | This study |
| *mshA*$^{F119S}$ | Fig. 5B, 5C, 5D | E7946 $Sm^R$, ΔVC1807::$Spec^R$, *mshA*$^{T70C, F119S}$ | HKQ030 (SAD3319) | This study |
| *mshA*$^{F119S}$ Δ*pilT* | Fig. 5B, 5C, 5D, S6B | E7946 $Sm^R$, ΔVC1807::$Spec^R$, *mshA*$^{T70C, F119S}$, Δ*pilT*::$Tm^R$ | HKQ036 (SAD3320) | This study |

| | | | | |
|---|---|---|---|---|
| $P_{BAD}$-*mshE* | Fig. S1A, S1B | E7946 $Sm^R$, ΔVC1807::$Cm^R$, *mshA*$^{T70C}$, Δ*mshE*::miniFRT, Δ*lacZ*::$P_{BAD}$-*mshE* $Carb^R$ | HKQ196 (SAD3321) | This study |
| $P_{BAD}$-*mshE* Δ*pilT* | Fig. S1A, S1B | E7946 $Sm^R$, ΔVC1807::$Cm^R$, *mshA*$^{T70C}$, Δ*mshE*::miniFRT, Δ*lacZ*::$P_{BAD}$-*mshE* $Carb^R$, Δ*pilT*::$Tm^R$ | HKQ496 (SAD3322) | This study |
| $P_{BAD}$-*dcpA* Δ*vps* | Fig. S1A, S1B | E7946 $Sm^R$, ΔVC1807::$Kan^R$, *mshA*$^{T70C}$, Δ*vps-rbmA*::$Zeo^R$, ΔVCA0692::$P_{BAD}$-*dcpA* $Carb^R$ | TND3247 (SAD3323) | This study |
| $P_{BAD}$-*dcpA* Δ*vps* Δ*pilT* | Fig. S1A, S1B | E7946 $Sm^R$, ΔVC1807::$Kan^R$, *mshA*$^{T70C}$, Δ*vps-rbmA*::$Zeo^R$, ΔVCA0692::$P_{BAD}$-*dcpA* $Carb^R$, Δ*pilT*::$Tm^R$ | HKQ494 (SAD3324) | This study |
| *mshE** | Fig. S1A, S1B | E7946 $Sm^R$, ΔVC1807::$Cm^R$, *mshA*$^{T70C}$, *mshE*$^{L10/54/58A}$ | SAD1756 | [23] |
| *mshE** Δ*pilT* | Fig. S1A, S1B | E7946 $Sm^R$, ΔVC1807::$Cm^R$, *mshA*$^{T70C}$, *mshE*$^{L10/54/58A}$, Δ*pilT*::$Tm^R$ | HKQ495 (SAD3325) | This study |
| $P_{BAD}$-*mshE** | Fig. S1A, S1B | E7946 $Sm^R$, ΔVC1807::$Cm^R$, *mshA*$^{T70C}$, Δ*lacZ*::$P_{BAD}$-*mshE*$^{L10/54/58A}$ $Carb^R$, Δ*mshE*::miniFRT | HKQ181 (SAD3326) | This study |
| $P_{BAD}$-*mshE** Δ*pilT* | Fig. S1A, S1B | E7946 $Sm^R$, ΔVC1807::$Cm^R$, *mshA*$^{T70C}$, Δ*lacZ*::$P_{BAD}$-*mshE*$^{L10/54/58A}$ $Carb^R$, Δ*mshE*::miniFRT, Δ*pilT*::$Tm^R$ | HKQ497 (SAD3327) | This study |
| *mshJ-mCherry* | Fig. S3 | E7946 $Sm^R$, ΔVC1807::$Spec^R$, *mshA*$^{T70C}$, *mshJ-mCherry* | TND3462 (SAD3328) | This study |
| *mshJ-mCherry* Δ*pilT* | Fig. S3 | E7946 $Sm^R$, ΔVC1807::$Spec^R$, *mshA*$^{T70C}$, *mshJ-mCherry*, Δ*pilT*::$Tm^R$ | TND3500 (SAD3329) | This study |
| *pilT*$^{WT}$ | Fig. S4A, S4B, S4C | E7946 $Sm^R$, ΔVC1807::$Kan^R$, *mshA*$^{T70C}$, ΔVCA0692::$P_{BAD}$-*mf-lon* CarbR | HKQ367 (SAD3330) | This study |
| *pilT-pdt2* | Fig. S4A, S4B, S4C | E7946 $Sm^R$, ΔVC1807::$Kan^R$, *mshA*$^{T70C}$, ΔVCA0692::$P_{BAD}$-*mf-lon* CarbR, *pilT*-pdt2 | HKQ368 (SAD3331) | This study |
| T25-PilT | Fig. S5 | TG1, pKT25-PilT $Kan^R$ | SAD2248 | [15] |
| T18-PilT | Fig. S5 | TG1, pUT18C-PilT $Carb^R$ | SAD2249 | [15] |
| T25-PilU | Fig. S5 | TG1, pKT25-PilU $Kan^R$ | SAD2250 | [15] |
| T18-PilU | Fig. S5 | TG1, pUT18C-PilU $Carb^R$ | SAD2251 | [15] |
| T25 E.V. | Fig. S5 | TG1, pKT25 vector $Kan^R$ | SAD2236 | [15] |
| T18 E.V. | Fig. S5 | TG1, pUT18C vector $Carb^R$ | SAD2240 | [15] |
| MshE-T25 | Fig. S5 | TG1, MshE-pKT25 $Kan^R$ | HKQ513 (SAD3332) | This study |
| MshE-T18 | Fig. S5 | TG1, MshE-pUT18C $Carb^R$ | HKQ515 (SAD3333) | This study |
| T25-PilB | Fig. S5 | TG1, pKT25-PilB $Kan^R$ | EHC052 (SAD3264) | [46] |
| T18-PilB | Fig. S5 | TG1, pUT18C-PilB $Carb^R$ | EHC050 (SAD3265) | [46] |
| T25-MshG | Fig. S5 | TG1, pKT25-MshG $Kan^R$ | SAD2272 | This study |
| T18-MshG | Fig. S5 | TG1, pUT18C-MshG $Carb^R$ | SAD2273 | This study |
| T25-Zip | Fig. S5 | TG1, pKT25-leucine zipper $Kan^R$ | SAD2238 | [15] |
| T18-Zip | Fig. S5 | TG1, pUT18C-leucine zipper $Carb^R$ | SAD2241 | [15] |
| $P_{tac}$-ribo-*mshA*$^{WT}$ Δ*pilT* | Fig. S7A, S7B, S7C | E7946 $Sm^R$, ΔVC1807::$Spec^R$, *mshA*$^{T70C}$, Δ*lacZ*::$P_{tac}$-riboswitch-*mshA*$^{T70C}$ $Kan^R$, Δ*pilT*::$Tm^R$ | HKQ493 (SAD3334) | This study |
| $P_{tac}$-ribo-*mshA*$^{P31S}$ Δ*pilT* | Fig. S7A, S7B, S7C, S7D | E7946 $Sm^R$, ΔVC1807::$Spec^R$, *mshA*$^{T70C}$, Δ*lacZ*::$P_{tac}$-riboswitch-*mshA*$^{T70C, P31S}$ $Kan^R$, Δ*pilT*::$Tm^R$ | HKQ106 (SAD3335) | This study |
| $P_{tac}$-ribo-*mshA*$^{WT}$ Δ*mshA* | Fig. S7C | E7946 $Sm^R$, ΔVC1807::$Spec^R$, *mshA*$^{T70C}$, Δ*lacZ*::$P_{tac}$-riboswitch-*mshA*$^{T70C}$ $Kan^R$, Δ*mshA*::miniFRT | HKQ113 (SAD3336) | This study |

| | | | | |
|---|---|---|---|---|
| $P_{tac}$-ribo-*mshA*$^{P31S}$ Δ*mshA* | Fig. S7C | E7946 $Sm^R$, ΔVC1807::$Spec^R$, *mshA*$^{T70C}$, Δ*lacZ*::$P_{tac}$-riboswitch-*mshA*$^{T70C, P31S}$ $Kan^R$, Δ*mshA*::miniFRT | HKQ112 (SAD3337) | This study |
| *mshA*$^{WT, T70C}$ $P_{tac}$-ribo-*mshA*$^{WT, T70}$ Δ*pilT* | Fig. S7D | E7946 $Sm^R$, ΔVC1807::$Spec^R$, *mshA*$^{T70C}$, Δ*lacZ*::$P_{tac}$-riboswitch-*mshA*$^{C70T}$ $Kan^R$, Δ*pilT*::$Tm^R$ | HKQ531 (SAD3338) | This study |
| *mshA*$^{WT, T70}$ $P_{tac}$-ribo-*mshA*$^{WT, T70C}$ Δ*pilT* | Fig. S7D | E7946 $Sm^R$, Δ*lacZ*::$P_{tac}$-riboswitch-*mshA*$^{T70C}$ $Kan^R$, Δ*pilT*::$Tm^R$ | HKQ529 (SAD3339) | This study |
| *mshA*$^{WT, T70C}$ $P_{tac}$-ribo-*mshA*$^{P31S, T70}$ Δ*pilT* | Fig. S7D | E7946 $Sm^R$, *mshA*$^{T70C}$, ΔVC1807::$Kan^R$, Δ*lacZ*::$P_{tac}$-riboswitch-*mshA*$^{P31S, C70T}$ $Cm^R$, Δ*pilT*::$Tm^R$ | HKQ526 (SAD3340) | This study |
| *mshA*$^{WT, T70}$ $P_{tac}$-ribo-*mshA*$^{P31S, T70C}$ Δ*pilT* | Fig. S7D | E7946 $Sm^R$, Δ*lacZ*::$P_{tac}$-riboswitch-*mshA*$^{P31S, T70C}$ $Kan^R$, Δ*pilT*::$Tm^R$ | HKQ533 (SAD3341) | This study |

863

864

865 **Table S2: Primer List**

| Primer name | Sequence (5' → 3') | Description |
|---|---|---|
| BBC1450 | CACTCAACGAGCTCAATACG | *mshA* F1 |
| BBC1453 | ATAGCCTTGCTGTTCATTTTGG | *mshA* R2 |
| ABD344 | GATTAGCAACGATTCTAGCGCAGGAG | ΔVC1807 F1 |
| ABD340 | gtcgacggatccccggaatACGTTTCATTAGTCACCTCTATTGT TAACTTGTTC | ΔVC1807 R1 |
| ABD341 | gaagcagctccagcctacaTAGTCGAAAATAAAAAAAAGAGG CTCGCCTC | ΔVC1807 F2 |
| ABD345 | CTTGCTAACCGTTGGTGTTACCAGC | ΔVC1807 R2 |
| DOG0400 | ACTTCTGGCTGAAGGTCAATTTTC | Δ*pilT/U* F1 |
| DOG0401 | gtcgacggatccccggaatCATTTAAATTCCTTAATAAAGTCTGGC | Δ*pilT* R1 |
| DOG0402 | gaagcagctccagcctacaTAGGTAGGTAAAGACAGATGGAG | Δ*pilT* F2 |
| DOG0403 | TCACGTGTTCGGCCAAAATC | Δ*pilT/U* R2 |
| ABD332 | GGCTGAACGTGGTTGTCGAAAATGAC | Δ*lacZ* F1 |
| ABD331 | GAACATGGGGTGTACGGCAGTGCtATTTAACGATGTGCGGG TTTTGCCAATCTTG | Δ*lacZ*::*lacIq* R1 |
| ABD255 | gaagcagctccagcctacaCCACAATAAGCCAGAGAGCCTTAAG | Δ*lacZ*::*lacIq* F2 |
| ABD256 | CCCAAATACGGCAACTTGGCG | Δ*lacZ* R2 |
| ABD841 | GGCACTGCCGTACACCCCATGTTCCGGTACCCGACACCATC GAATG | Amplify *lacIq* F |
| ABD842 | GGCTCTCTGGCTTATTGTGGGGGGAAACCTGTCGTGCCAGC TGC | Amplify *lacIq* R |
| BBC374 | TGGCAAAAAGCGAGAGAAGAAG | Δ*luxO* F1 |
| BBC375 | gtcgacggatccccggaatCATGAGGACATATTTTGTTTTCTGC | Δ*luxO* R1 |
| BBC376 | gaagcagctccagcctacaTAAGCGATGAGAGAATGGATCAAC | Δ*luxO* F2 |
| BBC377 | TCACACCCGAATTTCCATCATGC | Δ*luxO* R2 |
| pilA S81C F | AAAACTAATATTGAAGATTATATTGCGACAGAAGGC TgTTTTCCTGCAACAACTGCAGG | *pilA*$^{S56C}$ F |
| pilA R2 | CATTAATCGCGGTTTCAAAGTGCA | *pilA*$^{S56C}$ R2 |
| ABD648 | AACTAAGCTGCTGCAGATTGTC | *mshE* F1 |
| DOG0409 | gtcgacggatccccggaatTTTATTAATTGGCACTTTGTGTCTC | Δ*mshE* R1 |
| BBC742 | attccggggatccgtcgacCTGCAGTTCagaagcagctccagcctaca | miniFRT F |
| BBC743 | tgtaggctggagctgcttctGAACTGCAGgtcgacggatccccggaat | miniFRT R |
| BBC1748 | gaagcagctccagcctacaGAACCGATTTATCTGTAGGAGTAG | Δ*mshE* F2 |
| DOG0420 | TGTGTAGTCTAACGTTTCAATGC | *mshE* R2 |
| BBC1723 | caatttcacacaggatcccgggAGGAGGTATTTAAATGGATATCGCTG AGTTAC | ΔVCA0692::$P_{BAD}$-riboswitch-*pilT* insert F |
| BBC1724 | tgtaggctggagctgcttcCTAAAATGCTTTTAAATCCAACTCG | ΔVCA0692::$P_{BAD}$-riboswitch-*pilT* insert R |
| DOG0405 | gtcgacggatccccggaatCATCTGTCTTTACCTACCTAAAATGC | Δ*pilU* R1 |
| DOG0406 | gaagcagctccagcctacaTAGCGATGGTTACTTTGTGCG | Δ*pilU* F2 |
| HQP0001 | GGGCTCGGGTgctTCGACGACCTTGGCG | *pilT*$^{K136A}$ R1 |
| HQP0002 | CGCCAAGGTCGTCGAagcACCCGAGCCC | *pilT*$^{K136A}$ F2 |
| HQP0009 | GAAACGTGGCGCTGCTGTaatGGCCAAGATACCGAGAAT | *mshA*$^{V27I}$ R1 |
| HQP0008 | ATTCTCGGTATCTTGGCCattACAGCAGCGCCACGTTTC | *mshA*$^{V27I}$ F2 |
| HQP0013 | GAAACGTGGCGCTGCTGTaaaGGCCAAGATACCGAGAAT | *mshA*$^{V27F}$ R1 |
| HQP0012 | ATTCTCGGTATCTTGGCCtttACAGCAGCGCCACGTTTC | *mshA*$^{V27F}$ F2 |

| | | |
|---|---|---|
| HQP0016 | TAAGAAACGTGGCGCcacTGTGACGGCCAAGAT | *mshA*$^{A29V}$ R1 |
| HQP0015 | ATCTTGGCCGTCACAgtgGCGCCACGTTTCTTA | *mshA*$^{A29V}$ F2 |
| HQP0019 | TTGCAGGTTTAAGAAACGagaCGCTGCTGTGACGGCCAA | *mshA*$^{P31S}$ R1 |
| HQP0018 | TTGGCCGTCACAGCAGCGtctCGTTTCTTAAACCTGCAA | *mshA*$^{P31S}$ F2 |
| HQP0022 | GCCTTGCAGGTTTAAGAAcagTGGCGCTGCTGTGACGGC | *mshA*$^{R32L}$ R1 |
| HQP0021 | GCCGTCACAGCAGCGCCActgTTCTTAAACCTGCAAGGC | *mshA*$^{R32L}$ F2 |
| HQP0025 | AGACGATTGCAACGCAATtgaCTCACTCGAAGTATCTAG | *mshA*$^{F119S}$ R1 |
| HQP0024 | CTAGATACTTCGAGTGAGtcaATTGCGTTGCAATCGTCT | *mshA*$^{F119S}$ F2 |
| BBC753 | atttcacacaggatcccgggAGGAGGTaacgtaATGGAATCTTATCTAA GTAAAAAAGTC | Δ*lacZ*::$P_{BAD}$-*dcpA* F insert |
| BBC754 | tgtaggctggagctgcttcTTAAGTCTCACTCATACCTGACAG | Δ*lacZ*::$P_{BAD}$-*dcpA* R insert |
| BBC1721 | caatttcacacaggatcccgggAGGAGGTCACAAAaTGCCAATTAATA AACTGC | Δ*lacZ*::$P_{BAD}$-*mshE** F insert |
| BBC1722 | tgtaggctggagctgcttcCTACAGATAAATCGGTTCAACC | Δ*lacZ*::$P_{BAD}$-*mshE** R insert |
| BBC2022 | TGCCGATCTCGTTTATGGACG | Δ*vps-rbmA* locus F1 |
| BBC2023 | gtcgacggatccccggaatTGCCATTTTGATTGCCTCTGG | Δ*vps-rbmA* locus R1 |
| BBC2024 | gaagcagctccagcctacaCAAAGAGAGCCTTATTAGGCTCTC | Δ*vps-rbmA* locus F2 |
| BBC2025 | TGAAAGAGGTTGCTCTAGAACTCG | Δ*vps-rbmA* locus R2 |
| BBC2975 | caatttcacacaggatcccgggaggaggtGGTACCATGAGTAAAAAAATC AAACTACC | ΔVCA0692::$P_{BAD}$-*mf-lon* insert F |
| BBC2918 | tgtaggctggagctgcttcTCCTACTCAGGAGAGCGTTCAC | ΔVCA0692::$P_{BAD}$-*mf-lon* insert R |
| BBC4364 | ACTCTCGGTAAACTTGCACG | *mshJ* F1 |
| BBC4365 | tccaccacttccacctgcACCACCGATAAACTCCTCTC | *mshJ*-X R1 |
| BBC4366 | gcaggtggagcaggtggaGGCAGTCGAGAGGAGTTTATC | *mshJ*-X F2 |
| BBC2950 | TCATGGTTTGCTCCATCCC | *mshJ* R2 |
| BBC1835 | gcaggtggaagtggtggaGTGAGCAAGGGCGAGGAGG | *mCherry* F |
| BBC1836 | gattgcagcTTACTTGTACAGCTCGTCC | *mCherry* R |
| BBC2975 | caatttcacacaggatcccgggaggaggtGGTACCATGAGTAAAAAAATC AAACTAC | *mf-lon* insert F |
| BBC2918 | tgtaggctggagctgcttcTCCTACTCAGGAGAGCGTTCAC | *mf-lon* insert R |
| BBC2927 | cttcgtttttgttcgccgcAAATGCTTTTAAATCCAACTCGATT | *pilT-pdt2* R1 |
| BBC2932 | gcggcgaacaaaaacgaagaaaacaccaacgaagtgccgacctttatgctgaacgc gggccaggcgaactacctgtctcaataagaagcagctccagcctaca | *pdt2* F |
| BBC2933 | tgtaggctggagctgcttcttattgagacaggtagttcgcctggcccgcgttcagataaa ggtcggcacttcgttggtgttttcttcgtttttgttcgccgc | *pdt2* R |
| DOG0402 | gaagcagctccagcctacaTAGGTAGGTAAAGACAGATGGAG | *pilT-pdt2* F2 |
| BBC2513 | gaagcagctccagcctacaGATCCCCGGGTACCTAAGTAAC | BACTH pKT25-X F |
| BBC2512 | tccacctgctccacctgcCTCTAGAGTCGACCCTGCAG | BACTH pKT25-X R |
| BBC2515 | gaagcagctccagcctacaCCGAGCTCGAATTCATCGATATAAC | BACTH pUT18C-X F |
| BBC2514 | tccacctgctccacctgcCTCTAGAGTCGACCTGCAG | BACTH pUT18C-X R |
| BBC2517 | gcaggtggaagtggtggaGATCCCCGGGTACCGAGC | BACTH X-pKT25/pUT18C F |
| BBC2516 | tccacctgctccacctgcCTCTAGAGTCGACCTGCAGG | BACTH X-pKT25/pUT18C R |
| JCP027 | gcaggtggagcaggtggaGATATCGCTGAGTTACTGGAATTTAG | BACTH TXX-PilT F |

| | | |
|---|---|---|
| BBC1724 | tgtaggctggagctgcttcCTAAAATGCTTTTAAATCCAACTCG | BACTH TXX-PilT R |
| BBC2434 | gcaggtggagcaggtggaGAGTTGAATCAATATCTGGATGG | BACTH TXX-PilU F |
| BBC1726 | tgtaggctggagctgcttcCTACTCCATATCAATCTTCACATTC | BACTH TXX-PilU R |
| HQP0355 | gcaggtggagcaggtggaCCAATTAATAAACTGCGTAAACG | BACTH MshE-TXX F |
| BBC2316 | tccaccacttccacctgcCAGATAAATCGGTTCAACCAAACC | BACTH MshE-TXX R |
| BBC2638 | gcaggtggagcaggtggaCTCACCAACCTTGTTGCTATC | BACTH TXX-PilB F |
| BBC2639 | tgtaggctggagctgcttcTTAAAAGTAGAGCACACGCTG | BACTH TXX-PilB R |
| BBC2526 | gcaggtggagcaggtggaGCGACGTTTTATTATCAGGG | BACTH TXX-MshG F |
| BBC2532 | tgtaggctggagctgcttcTTAGCCCTTGAGTGCATCCATC | BACTH TXX-MshG R |
| BBC2617 | cctgctaaggaggtaacaacaagATGGTAATAATGAAAAGACAAGGTG | Δ*lacZ*::$P_{tac}$-riboswitch-*mshA* insert F |
| BBC1712 | tgtaggctggagctgcttcTTATTGCGCTGGTTTACCAC | Δ*lacZ*::$P_{tac}$-riboswitch-*mshA* insert R |
| ABD653 | gtcgacggatccccggaatCATCTCTCTTTCATGTGAATACGCA GC | Δ*mshA* R1 |
| ABD654 | gaagcagctccagcctacaGCGCAATAATTTAAATATGGCTCG TGC | Δ*mshA* F2 |
| HQP0129 | GTATATGCTGTGTAGTCTAAcgtTTCAATGCCTTTAATTGCAG | *mshA*$^{C70T}$ R1 |
| HQP0130 | CTGCAATTAAAGGCATTGAAacgTTAGACTACACAGCATATAC | *mshA*$^{C70T}$ F2 |

866

867